

CRISPR-Cas13d induces efficient mRNA knock-down in animal embryos

Gopal Kushawah¹, Luis Hernandez-Huertas^{2,3}, Joaquin Abugattas-Nuñez del Prado^{2,3,4}, Juan R. Martinez-Morales², Michelle L. DeVore¹, Huzaifa Hassan¹, Ismael Moreno-Sanchez^{2,3}, Laura Tomas-Gallardo⁵, Alejandro Diaz-Moscoso⁵, Dahiana E. Monges^{2,3}, Javier R. Guelfo^{2,3}, William C. Theune⁶, Emry O. Brannan⁶, Wei Wang¹, Timothy J. Corbin¹, Andrea M. Moran¹, Alejandro Sánchez Alvarado^{1,7}, Edward Málaga-Trillo⁴, Carter M. Takacs⁶, Ariel A. Bazzini^{1,8,*}, Miguel A. Moreno-Mateos^{2,3,9,*}

1 Stowers Institute for Medical Research, 1000 E 50th St, Kansas City, MO 64110, USA

2 Andalusian Center for Developmental Biology (CABD), Pablo de Olavide University/CSIC/Junta de Andalucía, Ctra. Utrera Km.1, 41013, Seville, Spain.

3 Department of Molecular Biology and Biochemical Engineer, Pablo de Olavide University, Ctra. Utrera Km.1, 41013, Seville, Spain.

4 Department of Biology, Universidad Peruana Cayetano Heredia, Av. Honorio Delgado 430, Lima 15102, Perú.

5 Proteomics and Biochemistry Unit, Andalusian Center for Developmental Biology/Pablo de Olavide University/CSIC/Junta de Andalucía. Ctra. Utrera Km.1, 41013, Seville, Spain

6 Department of Biology and Environmental Science, University of New Haven, West Haven, Connecticut 06516, USA.

7 Howard Hughes Medical Institute, Stowers Institute for Medical Research, Kansas, MO, USA.

8 Department of Molecular and Integrative Physiology, University of Kansas Medical Center, 3901 Rainbow Blvd, Kansas City, KS 66160, USA

9 Lead contact

*To whom correspondence should be addressed:

E-mail: mamormat@upo.es, arb@stowers.org

Tel: +34 954349210; +1 816-926-4113

Fax: +34 954349376; +1 816-926-4113

Keywords: CRISPR-Cas13, embryogenesis, zebrafish, RNA targeting

Running Title: CRISPR-RfxCas13d as RNA targeting tool in embryos

Summary

Early embryonic development is driven exclusively by maternal gene products deposited into the oocyte. Although critical in establishing early developmental programs, maternal gene functions have remained elusive due to a paucity of techniques for their systematic disruption and assessment. CRISPR-Cas13 systems have recently been employed to degrade RNA in yeast, plants and mammalian cell lines. However, no systematic study of the potential of Cas13 has been carried out in an animal system. Here, we show that CRISPR-RfxCas13d (CasRx) is an effective and precise system to deplete specific mRNA transcripts in zebrafish embryos. We demonstrate that zygotically-expressed and maternally-provided transcripts are efficiently targeted, resulting in a 76% average decrease in transcript levels and recapitulation of well-known embryonic phenotypes. Moreover, we show that this system can be used in medaka, killifish and mouse embryos. Altogether our results demonstrate that CRISPR-RfxCas13d is an efficient knock-down platform to interrogate gene function in animal embryos.

Introduction

The experimental dissection of gene function has been radically transformed with the advent of DNA engineering technologies such as TALEN and CRISPR-Cas9 systems (Hsu et al., 2014). These tools allow researchers to link genotype to cellular phenotype through the generation of permanent changes to the genome.

Complementary 'knock-down' approaches such as RNA interference have also proven to be invaluable tools to interrogate gene function. However, in aquatic vertebrate organisms such as zebrafish (*Danio rerio*), other teleost fish and *Xenopus* (Chen et al., 2017; Lund et al., 2011), attempts to establish efficient RNAi technologies have largely failed (Chen et al., 2017; Kelly and Hurlstone, 2011; Lund et al., 2011). In their place, morpholinos (MOs), and more recently, antisense oligonucleotides (ASOs), have been used to perturb RNA activity (Pauli et al., 2015; Stainier et al., 2017). While an ASO-based approach has not been followed up since its implementation in zebrafish (Pauli et al., 2015), MOs have been widely implemented for over two decades. MOs are nucleic acid-analog antisense oligomers that disrupt RNA function/output by blocking translation or splicing (Stainier et al., 2017). However, the utility of MOs has recently been called into question due to observed toxicity and off-target effects (Gentsch et al., 2018; Joris et al., 2017; Kok et al., 2015; Lai et al., 2019; Robu et al., 2007; Schulte-Merker and Stainier, 2014). In several instances, discordant phenotypes have been observed between MO-treated animals and loss-of-function mutant animals and, more strikingly, additional phenotypes have been observed upon MO treatment in loss-of-function mutant backgrounds, indicating cellular effects unrelated to targeted RNA knock-down (Joris et al., 2017; Kok et al., 2015). More recently, studies have shown that some MOs

can trigger an innate immunity response, activation of interferon and cellular stress response pathways, as well as off-targeting through mis-splicing in zebrafish and *Xenopus* (Gentsch et al., 2018; Joris et al., 2017; Lai et al., 2019; Robu et al., 2007), reinforcing the need for established controls to ensure the fidelity of MO-induced phenotypes (Stainier et al., 2017). These concerns, as well as the high expense of morpholinos, tedious methods for validating efficacy and fidelity (i.e. assessment of protein output or ribosome occupancy) (Lee et al., 2013), and the inability to implement in a tissue-specific or temporal manner, have limited their use in systematic approaches to studying gene function in teleost and amphibian embryos.

RNA 'knock-down' approaches hold many advantages compared to DNA mutagenesis (e.g. Cas9). The ability to directly disrupt gene activity sidesteps the need for laborious multi-generation genotype screening to establish permanent genetic strains. Likewise, knock-down strategies allow for the study of *in vivo* maternal effects without the need for homozygous mutant mothers (Ciruna et al., 2002; Moreno-Mateos et al., 2015), which for many critically important genes are either unviable or infertile (Abrams and Mullins, 2009; Ciruna et al., 2002). Furthermore, by directly manipulating RNA activity in a relatively tunable manner, researchers can study how subtle changes in transcript levels impact biological processes. In fact, by reducing but not completely removing gene activity, researchers can uncover phenotypes that may otherwise remain hidden due to loss-of-function lethality (Smith et al., 2017). Finally, therapeutic approaches that target RNA rather than DNA can be advantageous in providing temporary but effective modifications without the prospect of permanent heritable changes (Cox et al., 2017).

Cas13 is a class 2/type VI CRISPR-Cas RNA endonuclease, which has recently been employed to induce both the cleavage and subsequent degradation of RNA in fission yeast, plants and mammalian cell lines (Abudayyeh et al., 2017; Aman et al., 2018; Cox et al., 2017; Jing et al., 2018; Konermann et al., 2018). This method has been shown to be more effective and specific than RNAi in mammalian cells (Abudayyeh et al., 2017; Cox et al., 2017; Konermann et al., 2018). However, to date, no systematic study of the potential of Cas13 has been carried out in an animal model system. Here, we show that CRISPR-RfxCas13d (CasRx), but not Psp/PguCas13b or LwaCas13a, is an effective and precise system to deplete specific mRNA transcripts in zebrafish embryos. We demonstrate that zygotically-expressed, as well as ectopic or maternally-provided transcripts are efficiently targeted, resulting in an average of more than 76% decrease in transcript levels and the recapitulation of well-known maternal and/or zygotic embryonic phenotypes. Importantly, through whole transcriptome sequencing, we observed specific knock-down of target mRNA. In addition, we show that the use of purified Cas13d protein increases maternal phenotype penetrance, while preserving the specificity observed with Cas13d mRNA. Finally, we successfully implement CRISPR-Cas13d system in other research organisms such as medaka (*Oryzias latipes*), killifish (*Nothobranchius furzeri*) and mouse (*Mus musculus*) embryos, demonstrating its applicability across a range of aquatic and terrestrial animal models. Our results establish CRISPR-Cas13d as an efficient and straight-forward method for the systematic, tractable, and unambiguous study of gene function *in vivo* during embryogenesis across a range of animal species.

Design

Gene knock-down approaches such as RNA interference serve an invaluable research tools toward elucidating gene function. However, in aquatic vertebrate organisms such as zebrafish and other teleost fish, RNA interference has failed to develop as an efficient and systematic tool. Instead, MOs have been used to disrupt gene function by blocking translation or preventing RNA splicing. However, MOs can induce nonspecific effects that are separate from target RNA perturbation (Gentsch et al., 2018; Joris et al., 2017; Lai et al., 2019; Robu et al., 2007). Further, researchers have found that MO-based phenotypes can differ from those obtained by genetic mutation (Kok et al., 2015). Although these differences may be explained, in part, by genetic compensation (El-Brolosy et al., 2019; Ma et al., 2019; Rossi et al., 2015), the use of MOs requires several proper controls to ensure accuracy (Stainier et al., 2017). Based on the limitations and caveats of current knockdown technologies in teleosts, we set out to develop and optimize a CRISPR-Cas13-based method to disrupt gene function. We had two goals: 1) develop an approach to interrogate maternally-provided developmental programs in the early embryo and 2) develop a technique that could be used in a systematic and cost-efficient manner. The study of early development in animal embryos, which is driven by thousands of mRNAs that are maternally provided (Lee et al., 2014), has traditionally required elaborate genetic schemes to remove maternal activity (Ciruna et al., 2002). Herein, we find that, among various Cas13 variants tested, RfxCas13d efficiently disrupts maternal and zygotic gene function without embryonic toxicity, and with specificity, in zebrafish embryos. Notably, Cas13d protein injection accelerates maternal RNA depletion and consequently provides more

penetrant phenotypes. Through successful application in medaka, killifish and mouse embryos, we find that CRISPR-RfxCas13d provides a fast, robust and cost-effective technology to systematically disrupt gene function in vertebrates. We envision the application of this method to the high-throughout study of gene expression in the early embryo, as well as in combination with inducible and tissue-specific methodologies.

Results

Optimization of RNA targeting by CRISPR-Cas13 in zebrafish embryos

To assess the potential toxic effects of different Cas13 proteins successfully used in mammalian cells (Abudayyeh et al., 2017; Cox et al., 2017; Konermann et al., 2018), we constructed expression vectors to generate comparable mRNA encoding four different Cas13 variants (*RfxCas13d*, *PguCas13b*, *PspCas13b* or *LwaCas13a-GFP*). The mRNA for each Cas13 variant was injected individually into one-cell stage zebrafish embryos (Figure 1A). Protein expression *in vivo* was confirmed for all Cas13 variants tested (Figure S1A) except *LwaCas13a-GFP* likely due to a low stability of *LwaCas13* mRNA as reported in mammalian cells (Abudayyeh et al., 2017) (Figure S1B). While *PguCas13b* and *PspCas13b* negatively impacted embryonic development (Figures 1B and S1C), *RfxCas13d* displayed no toxic effects (up to 300 pg of mRNA per embryo; Figure S1D). Hence, we limited subsequent analyses of endogenous mRNA abrogation to *RfxCas13d*. First, to test whether *RfxCas13d* could trigger the degradation of specific mRNAs in zebrafish embryos, we designed and generated six guide RNAs (gRNAs) complementary to different sequences within the coding sequence (CDS) of the *tbxta* mRNA pooled into 2 sets of gRNAs (Figures 1C, S1E and S1F). Notochord formation is compromised in *tbxta* loss-of-function mutant embryos as well as a lack of posterior

structures (no-tail) (Halpern et al., 1993; Schulte-Merker et al., 1994). Co-injection of *RfxCas13d* mRNA (mCas13d) with different sets of *tbxta* gRNAs (Figure 1C) recapitulated the no-tail phenotype at 30 hours post injection (Figures 1D, 1E, S1G and S1H) (Strahle et al., 1996) and persist for at least 4 days post injection (Figure S1I). Importantly, the no-tail phenotype was only observed when *tbxta* gRNAs and mCas13d were co-injected (i.e., no phenotype was observed when either gRNAs or mCas13d were injected singly) and its penetrance correlated with mCas13d dosage (Figure 1E). Additionally, chemically synthesized (Synt) gRNAs generated a similar number of *no tail* embryos but with a slight increase in phenotype penetrance (Figure S1J). Further, co-injection of mCas13d with gRNAs targeting *dnd1*, a gene controlling an unrelated developmental process (germ cell development and survival) (Weidinger et al., 2003), did not produce a *no tail* phenotype (Figure 1F). In addition, the CRISPR-RfxCas13d system triggered *tbxta* mRNA degradation by at least 6 hours post injection (Figure 1G) ($p < 0.003$, t-test). While the addition of nuclear localization sites (NLS) increased RfxCas13d activity in mammalian cells (Konermann et al., 2018), we observed that incorporation of an NLS decreased phenotypic penetrance in zebrafish embryos (Figure S1K) ($p < 3.4e-9$, Chi-Square). Finally, to confirm the specificity of the phenotype, we designed a new set of three gRNAs targeting the *tbxta* 3'UTR which also induced the no-tail phenotype (Figure 1F). This phenotype was partially rescued ($p < 2.07e-3$, Chi-Square) by injection of the cognate mRNA (lacking endogenous 3'UTR), but not by injection of mRNA encoding GFP or the antisense *tbxta* coding region ($p < 0.02$ and 0.29 , respectively; Chi-Square) (Figures 1F and S1L). To test the ability of targeting of individual gRNAs, we injected Cas13d mRNA together with nine individual and different

gRNAs targeting *tbxta* mRNA and observed that all of them recapitulated the *no tail* phenotype with variable penetrance (Fig. S1M). All together, these results establish CRISPR-RfxCas13d as an efficient tool to trigger endogenous mRNA knock-down during zebrafish embryogenesis.

CRISPR-RfxCas13d triggers effective and precise reporter mRNA depletion in zebrafish embryos

To further assess the efficacy of the CRISPR-RfxCas13d system to impair mRNA activity, two sets of three gRNAs each, specific to the CDS of either Red Fluorescent Protein (RFP) or Nano-luciferase, were individually injected together with their corresponding controls (*gfp* and *firefly* mRNAs, respectively) along with mCas13d into zebrafish embryos (Figures 2A and B). Reporter activity (Figures 2C and D), as well as the respective mRNA levels (Figures 2E and F), were significantly reduced in zebrafish embryos after 6 hours post injection when compared to embryos injected with control conditions (Figures 2C-F). Moreover, mCas13d coupled with individual gRNAs was sufficient to reduce RFP fluorescence intensity (Figure S2A and S2B). Notably, fluorescence intensity of Green Fluorescent Protein (GFP) and Firefly, respectively, did not decrease appreciably in all conditions tested (Figures 2C, S2A, S2B and S2C), and only targeted mRNAs (*rfp* and *nano-luciferase*) displayed reduced mRNA levels (Figures 2C-F and S2A,B), suggesting that the CRISPR-RfxCas13d system is specific.

To address whether the CRISPR-RfxCas13d system could be used to target maternally deposited mRNAs, zebrafish embryos derived from a transgenic mother that expresses *rfp* at very high levels (i.e. among the top 100 most highly expressed

maternal mRNAs) were injected with mCas13d, *gfp* mRNA, plus three gRNAs targeting *rfp* (Figure 2G). Fluorescence intensity was visibly reduced after 24 hours post injection when compared to embryos injected with mCas13d or gRNAs alone, or by co-injection of mCas13d with unrelated gRNAs (Figure 2H). Interestingly, the reduced level of RFP persisted for the first 3.5 days and partially recovered after 5 days (Figures S2D and S2E, respectively). Furthermore, *rfp* mRNA levels displayed an approximately 4.4 fold reduction (77.3 %; p adjusted < 7.64e-6) compared to embryos injected with mCas13d alone after 6 hours post injection by RNA-seq (Figure 2I) and qRT-PCR (Figure S2F). Moreover, RNA-seq analysis displayed similar transcript levels in zebrafish embryos injected with mCas13d alone or uninjected embryos (Figures 2I and S2G). Importantly, within the co-injected embryos with mCas13d and gRNAs targeting *rfp* mRNA, *rfp* was the most significantly down-regulated transcript (with more than >4 fold change) (Figures 2I and S2G). Together, these results indicate that the CRISPR-RfxCas13d system can functionally disrupt the activity of maternally provided mRNAs in a specific manner during early development in zebrafish embryos.

CRISPR-RfxCas13d system efficiently depletes maternally provided and zygotically-expressed mRNAs in zebrafish embryos

We next set out to assess the efficacy and specificity of targeted gene knockdown on both maternally-provided and/or zygotically expressed mRNAs in zebrafish embryos. To assess transcriptome-wide effects after endogenous gene knockdown, we targeted the *szrd1* mRNA. No loss-of-function phenotype has been reported for *szrd1*, and we observed no developmental abnormalities during the first 6

hours post injection (Figure 3A). However, *szrd1* mRNA levels showed a 7-fold reduction in expression (p adjusted $< 3.4e-10$) compared to embryos injected with mCas13d alone (at 6 hpi), with no other substantial mRNA changes observed (Figures 3B and S3A).

We next tested our optimized CRISPR-RfxCas13d method on endogenous mRNAs with known roles in embryonic development and previously characterized loss-of-function phenotypes. First, we targeted *dnd1* mRNA, whose impairment abolishes primordial germ cell migration and survival (Weidinger et al., 2003). Embryos co-injected with mCas13d and 3 gRNAs targeting *dnd1* were devoid of detectable germ cells, as indicated by loss of germ cell-specific GFP expression (co-injection of GFP-nanos 3'UTR (Ciruna et al., 2002; Weidinger et al., 2003) (Figure 3C). In contrast, germ cells were not visibly affected by injection of mCas13d alone or in conjunction with gRNAs targeting an unrelated mRNA (Figure 3C). RNA-seq and qRT-PCR analysis confirmed specific reduction (8-fold change -87.5%-, p adjusted $< 2.76e-6$, RNAseq) of *dnd1* mRNA levels (Figures 3D and S3B). Notably, *dnd1* mRNA was the most differentially expressed mRNA (at 6 hpi) when compared to embryos injected with mCas13d alone (Figures 3D and S3C).

Nanog is a potent transcription factor involved in the activation of zygotic gene expression in zebrafish (Gagnon et al., 2018; Lee et al., 2013; Veil et al., 2018) and injection of morpholinos targeting *nanog* mRNA or maternal and zygotic (MZ) loss-of-function induces severe gastrulation deficiencies and epiboly failure in zebrafish embryos (Lee et al., 2013; Veil et al., 2018). In a similar manner, embryos injected with mCas13d and three gRNAs targeting *nanog* mRNA displayed a significant reduction in

nanog mRNA levels at 6 hours post injection (6-fold change, 84%, p adjusted $< 3.536 \times 10^{-9}$, RNAseq) (Figures 3F, S3F and S3G) and related gastrulation defects (Figures 3E, S3D and S3E), which were also observed after injection of mCas13d with individual *nanog* gRNAs (Figure S3H). Importantly, downstream gene expression changes were similar to those reported in *nanog* MO-treated embryos (Gagnon et al., 2018; Lee et al., 2013) (*nanog* targets; Figure 3F). Specifically, mRNAs downregulated in embryos injected with mCas13d plus *nanog* gRNAs (139 mRNAs, $p < 1 \times 10^{-4}$, fold change > 2) were also downregulated in *nanog* morpholino-treated embryos (Lee et al., 2013) ($p < 4.4 \times 10^{-11}$, Wilcoxon rank sum test) (Figures S3G and S3I). Conversely, mRNAs that displayed a greater than 4-fold reduction in *nanog* MO-treated embryos were also repressed after co-injection of mCas13d and *nanog* gRNAs ($p < 1.7 \times 10^{-5}$, Wilcoxon rank sum test) (Figure 3F). Thus, given the strong correspondence between MO and CRISPR-RfxCas13d methods, affected mRNAs are likely true targets of *nanog* (both direct and indirect).

Recent studies indicate that LwaCas13a in glioma cells can exhibit nonspecific *trans*-RNA cleavage activity, also called ‘collateral’ activity (Abudayyeh et al., 2016; Wang et al., 2019). In contrast, we observed high and consistent RNA integrity numbers (RIN) across all samples (e.g. untreated, mCas13d-treated, and mCas13d plus gRNA-treated), suggestive of undetected collateral activity ($p > 0.08$; One-way ANOVA) (Figure S3J). Moreover, we also did not observe activation of stress and immune system responses upon treatment with mCas13d plus gRNAs, a concern associated with morpholino-based knockdown approaches (Figure S3K) (Lai et al., 2019). Finally, mRNAs that could be recognized allowing up to 4 mismatches by any of the used

gRNAs, were not substantially affected (Figure S2G and S3A, C and G). Taken together, our results suggest that CRISPR-RfxCas13d system is specific.

Encouraged by these results, we targeted additional genes with previously characterized phenotypes. RfxCas13d-mediated reduction in *smad5* or *alk8* mRNA levels led to whole body dorsalization (Bauer et al., 2001; Bellipanni et al., 2006; Laux et al., 2011) while reductions in *oep* or *smad2* mRNA resulted in ventralization or curved dorso-ventral phenotypes, consistent with previous reports (Dubrulle et al., 2015; Nasevicius and Ekker, 2000; Pauli et al., 2015) (Figure 3G and S3L). Finally, injection of mCas13d with 3 gRNAs targeting *PrP-1* mRNA, one of the two zebrafish orthologues of the mammalian prion protein, recapitulated early epibolic arrest after MO treatment (Malaga-Trillo et al., 2009; Sempou et al., 2016) (Figure S3M).

To test whether the CRISPR-RfxCas13d system can reduce transcript levels of developmental genes expressed later in development, we designed three gRNAs targeting the tyrosinase (*tyr*) mRNA involved in pigmentation whose transcription starts at 16-17 hours post fertilization (Camp and Lardelli, 2001). Embryos injected with *tyr* gRNAs and mCas13d displayed reduced pigmentation in both eye and body when compared to embryos injected with either mCas13d or *tyr* gRNAs alone (Figures 3H and S3N). Interestingly, as we observed for *rfp* mRNA above, pigmentation was partially restored after 3.5 days post injection (Figure S3N), consistent with decreased activity over time post-injection. Similar decreased pigmentation was observed after injection of mCas13d with 8 individual and different gRNAs (Figure S3O) but with variable penetrance.

Finally, it has recently been shown that genetic compensation can be triggered by RNA degradation for some mRNAs (El-Brolosy et al., 2019; Ma et al., 2019). Interestingly, in zebrafish embryos co-injected with three gRNAs and mCas13d targeting *vc1a*, we observed significantly reduced levels of *vc1a* mRNA but increased expression of its paralog, *vc1b* (Fig S3P). Taken together, these results demonstrate that CRISPR-RfxCas13d efficiently induces maternal and zygotic mRNA knockdown, recapitulates early embryogenesis phenotypes in zebrafish embryos, and is associated with minimal toxicity, off-targeting, and stress or immune response activation.

Injection of RfxCas13d protein targets maternal mRNA faster and provides higher phenotypic penetrance in zebrafish embryos.

Injection of mCas13d requires time for the embryo to generate RfxCas13d protein (Cas13d protein), potentially delaying knockdown activity. Therefore, we hypothesized that injection of purified Cas13d protein may lead to more rapid maternal mRNA depletion (and potentially more penetrant phenotypes; Figure 4A). Minimal toxicity was observed upon injection of purified Cas13d protein (up to 3 ng; Figures S4A, B and C). Co-injection of the Cas13d protein with three *nanog* gRNAs, recapitulated the *nanog* maternal phenotype in a Cas13d dose-dependent manner (Figures 4B and 4SD). Compared to mCas13d, co-injection of three *nanog* gRNAs with Cas13d protein resulted in greater depletion (~70%) of *nanog* mRNA at 2 hours post injection (Figure 4C), and significantly more embryos with severe gastrulation and epiboly defects (Figure 4B) ($p < 4.8e-12$, Chi-Square, lane 6 to 9). Increased penetrance was also observed with synthesized (Synt) gRNAs when compared to *in vitro*

transcribed gRNAs (Figure 4B) ($p < 0.03$, Chi-Square, lane 6 to 7) for both *nanog* and *no-tail* phenotypes (Figure S1J). Similarly, injection of high amount of gRNAs (1 ng) did not display toxicity but increased phenotype penetrance (Figure 4B) ($p < 0.005$, Chi-Square, lane 10 to 11). To analyze the specificity of Cas13d protein, we further targeted two early-expressed developmental genes *dnd1* and *szrd1*. Targeting of *dnd1* recapitulates the depletion of germ cells phenotype (Figure 4D), while *szrd1* does not show any phenotype by 6 hpi (Figure 4E) as observed for mCas13d (Figure 3C and A), respectively. Our RNA-seq data indicates that *dnd1* and *szrd1* were the most down-regulated genes (6.9 and 6.3 fold change, p adjusted $< 2e-3$ and $< 7.43e-14$, respectively) (Figures 4F and Figures 4SE and F), consistently with our RNA-seq data using mCas13d (Figure S4G). Although we cannot discriminate between off-targeting and downstream consequences of knock-down, we did not observe changes in expression of genes that possessed potential target sites (due to slightly mismatched gRNA:target complementarity) (Figures 4SE and F). Furthermore, using purified Cas13d protein we observed neither stress or immune response nor collateral activity (Figures S4H and I) as we have shown for mCas13d injections. Altogether, our results demonstrate that Cas13d protein injection is a robust approach to induce RNA depletion in a specific manner but further accelerates RNA degradation kinetics *in vivo* when compared to mCas13d.

Encouraged by our results, we sought to uncover novel roles for early developmental genes in zebrafish. The Bromodomain and Extraterminal (BET) protein family (Brd: Brd2, Brd3 and Brd4 proteins) have been recently implicated in zygotic genome activation (ZGA) via recognition of chromatin acetylation. Specifically,

pharmacologic inhibition (JQ1) of BET proteins (Brd2-4) and overexpression of *brd4* together with P300 delay and accelerate ZGA, respectively (Chan et al., 2019). However, the individual roles and contributions of different Brd factors to this process remain unclear. The top three highly maternally-contributed and translated (before ZGA) *brd* mRNAs, *brd4*, *brd3a* and *brd3b* (Bazzini et al., 2014; Chan et al., 2019), were individually knocked-down after co-injection of three gRNAs with Cas13d protein (Figure 4G). Interestingly, *brd4* and *brd3a* but not *brd3b* showed a developmental phenotype ($p < 6.26 \times 10^{-11}$, $p < 5.08 \times 10^{-9}$, $p = 0.677$, Chi-Square, respectively) similar to that observed after *nanog* mRNA knock-down or using JQ1 (Chan et al., 2019), suggesting that the depletion of *brd4* and *brd3a* alters ZGA (Figure 4H). In addition, we measured mRNA levels of three early expressed genes whose transcription depends on Brd activity (Chan et al., 2019) and two of them were significantly down-regulated when *brd4* was targeted by CRISPR-RfxCas13d (Figure 4SJ) suggesting that *brd4* controls their expression at the molecular level. Finally, similar to our previous *nanog* knock down experiments, we observed higher phenotypic penetrance when *brd4* was targeted using Cas13d protein compared to mCas13d (Figure S4K) ($p < 0.05$ Chi-Square, lane 3 vs 4). These results suggest that maternal *brd3a* and *brd4* mRNAs are involved in zebrafish zygotic genome activation and highlight the use of purified Cas13d protein to interrogate maternal factors functions.

Altogether, our data show that the CRISPR-RfxCas13d system is a precise tool to impair maternal and early zygotic gene activity in zebrafish embryos, resulting in an efficient reduction in target mRNA abundance (Figure S4L).

CRISPR-RfxCas13d as RNA targeting tool in different animal models

To determine how the CRISPR-RfxCas13d system performs in other animal models, we first assessed its activity in medaka, another fish model for which RNAi is ineffective (Chen et al., 2017). Loss-of-function mutations in the *rx3* (*rax*) gene result in arrested eye development (Loosli et al., 2001). Co-injection of mCas13d plus three gRNAs targeting the *rx3* mRNA into one-cell stage medaka embryos resulted in *rx3* mRNA depletion (Figure S5A) (uninjected or mCas13d alone vs mCas13d and gRX3, $p < 0.011$; One-way ANOVA), and severe microphthalmia and/or anophthalmia, which were not observed with injection of mCas13d alone (Figures 5A, S5B and S5C) ($p < 2.7 \times 10^{-12}$, Chi-Square). Next, we assessed the ability of mCas13d to disrupt reporter mRNA activity in the killifish (*Nothobranchius furzeri*), a research organism used to study aging and regeneration. We introduced mRNAs encoding *gfp*, *rpf*, mCas13d, as well as three gRNAs targeting *rpf*. We observed a reduction in *rpf* mRNA level and fluorescence intensity 14 hours post injection when compared to control embryos (i.e. mCas13d or gRNAs alone; Figures 5B, S5D and S5E). Together, these results suggest that the CRISPR-RfxCas13d system can be widely applied across several animal species, including those historically recalcitrant to RNAi-based knock-down methodologies (e.g. zebrafish, medaka and killifish) (Chen et al., 2017).

Although CRISPR-Cas13 has been shown to be effective in cultured mammalian cells, its efficacy has, to date, not been determined in mammal embryos. Therefore, we next assessed potential toxic effects of increasing concentrations of mCas13d in one-cell stage mouse embryos. We find that up to 1-2 μ l of 25 ng/ μ l of mCas13d is tolerated with no deleterious effects (Figures S5F and S5G). Importantly, we observed lower RFP

fluorescence intensity at 2-cell stage when mCas13d was co-injected with *rfp* mRNA and respective gRNAs, compared to mouse embryos injected with either mCas13d or *rfp* gRNAs alone, as well as in the presence of mCas13d plus three unrelated gRNAs targeting the *Danio rerio tyr* gene (Figure 5C and 5SH). To assess the effects on endogenous gene activity, we designed gRNAs targeting *ubtf* and *emg1* mRNAs. In both cases, introduction of mCas13d plus respective pools of gRNAs resulted in developmental arrest ($p < 0.011$ and $p < 3.5e-05$, respectively compared to mCas13d alone; Chi-Square) (Figure 5D), similar to previously observed phenotypes in loss-of-function mutant embryos (Hamdane et al., 2014; Wu et al., 2010). Together, these results suggest that the CRISPR-RfxCas13d system can serve as an effective additional knock-down tool in mice embryos.

Discussion

The ability to experimentally modulate gene activity is critical for understanding biological function. In this study, we show that the CRISPR-RfxCas13d system provides a robust, highly efficient, specific and straight-forward method to disrupt mRNA function in a wide variety of embryonic animal models.

A CRISPR-Cas-based system for perturbing RNA function has several advantages. Foremost, as shown here, Cas13-mediated knock-down can be applied to teleost fish models in which current RNAi methodologies remain ineffective (Chen et al., 2017; Kelly and Hurlstone, 2011). The CRISPR-Cas13 system does not burden endogenous cellular machinery. This is of particular concern in aquatic vertebrates such as *Xenopus*, where the sequestration of Argonaute proteins by exogenous RNAi is

thought to compromise endogenous microRNA function (Kelly and Hurlstone, 2011; Lund et al., 2011). Another advantage lies in the ease, flexibility, and cost-effectiveness of this approach. Researchers can generate gRNAs and mCas13d through conventional *in vitro* transcription reactions. Alternatively, synthetic gRNAs and/or purified Cas13d protein can be used, resulting in more penetrant maternal phenotypes, presumably due to earlier activity post-injection. Since RfxCas13d does not have nucleotide sequence restrictions or protospacer flanking site (PFS) requirements in eukaryotic cells (Abudayyeh et al., 2017; Cox et al., 2017; Konermann et al., 2018), any sequence can be potentially targeted, including untranslated regions, alternative splice sites, as well as long non-coding RNAs. Because mRNA levels are directly impacted by targeted degradation (in contrast to most MO-based strategies), validation can be performed via Northern blot analysis, quantitative RT-PCR, or RNA-seq. Importantly, we observed no interferon or stress response in treated embryos (Lai et al., 2019). On the other hand, we observed some transcriptomic noise, particularly after injection of Cas13d protein. We speculate that this molecular effect could be due to the high amount of mRNA or protein injected, and/or CRISPR-Cas injections in zebrafish embryos. However, we do not observe toxicity, nonspecific developmental abnormalities, direct off-targets (up to 4 mismatches between gRNA and target) or collateral activity after targeted knockdown. We conclude that tested conditions do not trigger a significant physiological response *in vivo* apart from expected developmental phenotypes. Further analysis will clarify whether this slight transcriptomic noise is specifically due to CRISPR-Cas transient injections in the embryo and can be diminished using lower amount and/or higher quality reagents such as synthetic gRNAs and purer RfxCas13d. In addition, we have

found that Cas13d performs better than a Cas13d variant with two nuclear localization signals (NLS; on N- and C-termini) in zebrafish embryos. However, we cannot rule out the possibility that NLS-containing versions will be more effective in other model animal systems or under transgenic expression, as has been shown in mammalian cells (Konermann et al., 2018). Finally, we have found that CRISPR-RfxCas13d may trigger genetic compensation in zebrafish embryos. While this is a single example, future work will examine how pervasive this response is upon Cas13-mediated knockdown, as well how gRNA positioning on the targeted mRNA influences this compensatory response (e.g. close to 5' or 3' end).

The ease and cost of Cas13-mediated knockdown will enable large-scale screening of maternal factors (both coding and noncoding) involved in early development. Additionally, transgenic lines expressing RfxCas13d, either ubiquitously, or in an inducible tissue or cell-specific manner, can be applied to the study of genes involved in development, as well as for targeting genes whose disruption results in early lethality or deleterious effects of ambiguous origins. In addition, this study will be a baseline to implement other CRISPR-Cas13 applications *in vivo* beyond induced RNA degradation such as RNA editing, transcript tracking and imaging optimized in mammalian cells (Cox et al., 2017; Konermann et al., 2018; Yang et al., 2019). Finally, the efficacy of Cas13-mediated knockdown in animals opens potential therapeutic opportunities to transiently target endogenous or viral RNAs as has been recently shown in transgenic plants (Mahas et al., 2019) and mammalian cell culture (Freije et al., 2019).

In sum, we have found that CRISPR-RfxCas13d system is adaptable and effective in a broad spectrum of animal models, and as such, will be an invaluable tool for unraveling gene function during development.

Limitations

We have shown that CRISPR-RfxCas13d can disrupt early developmental programs by targeting maternal mRNAs. However, as with other knock-down techniques in teleost embryos, this approach cannot target maternally provided protein. In addition, we have found variable gRNA activity as has been shown for other CRISPR-Cas systems *in vivo* (Moreno-Mateos et al., 2017; Moreno-Mateos et al., 2015). Indeed, a CRISPR-RfxCas13d activity prediction tool for gRNA has been recently developed in mammalian cell culture (Wessels et al., 2020). However, CRISPR-Cas targeting activity varies between *ex vivo* and *in vivo* approaches (Haeussler et al., 2016), highlighting the need for additional prediction algorithms for selecting the most efficient gRNAs *in vivo*.

Finally, although *in vivo* viral delivery of RfxCas13d in mice (Zhou et al., 2020) as well as transgenic expression of RfxCas13d in plants (Mahas et al., 2019) has been recently demonstrated to be efficient and safe, a recent preprint has shown that RfxCas13d-NLS can have toxic effects in transgenic flies when expressed under the control of strong promoters (constitutive or tissue-specific) (Buchman et al., 2020). Although such toxicity may be specific to *Drosophila*, we cannot rule out the possibility that high and sustained RfxCas13d activity will be deleterious in other contexts, thus potentiating the need for controlled transgenic expression studies.

Acknowledgements

We thank Raktim Roy and Kai Zhang and Hui Qian for initial support, Fish facility, Molecular Biology facility and Shiyuan Chen from the Computational core facilities from Stowers Institute and Ana Fernández-Miñan from the CABD genomic and Genetics section within the Department of Molecular Biology and Biochemical Engineer at University Pablo de Olavide for reagents and experimental support. We also thank Paul Trainor and Michael Durnin for their help with mouse experiments, Mark Miller and Philippe Noguera for illustrations and animations and Juan P. Fernandez for critical reading of the manuscript. We thank Ignacio Maeso (CABD) and Alfonso Fernandez-Alvarez (CABD) and all members of the Moreno-Mateos and the Bazzini laboratories for intellectual and technical support. This work was supported by Ramon y Cajal program (RyC-2017-23041) and grants PGC2018-097260-B-I00 and MDM-2016-0687 from Spanish Ministerio de Ciencia, Innovación y Universidades and the Springboard program from CABD (M.A.M-M) and the Stowers Institute for Medical Research (A.A.B). M.A.M-M was recipient of the Genome Engineer Innovation 2019 Grant from Synthego. A.A.B was awarded with Pew Innovation Fund. J.R.M-M is supported by BFU2017-86339-P and MDM-2016-0687 grants (Spanish Ministerio de Ciencia, Innovación y Universidades). E. M-T and J.A.-NP are supported by INNOVATE PERÚ grant 168-PNCP-PIAP-2015 and FONDECYT travel grant 043-2019. The CABD is an institution funded by Pablo de Olavide University, Consejo Superior de Investigaciones Científicas (CSIC) and Junta de Andalucía.

Author contributions

M.A.M.-M. and A.A.B. conceived the project and designed the research. M.A.M.-M., G. K., A.A.B., L.H-H. and J.A.-NP. performed all zebrafish experiments with the contribution of M.D.V., I. M-S. and J.R.G. W.C.T. and E.O.B. carried out CRISPR-LwaCas13a experiments and *shh in situ* experiments. L.T-G., A.D-M. and D.C.M purified RfxCas13d protein. J.R.M-M. M.A.M.-M and J.A.-NP. performed medaka experiments. W.W, T.J.C, A.M.M and G.K carried out killifish and mouse experiments. H.H did primary RNA-seq analysis. E.M-T. and A.S.A. provided reagents and materials. M.A.M.-M., A.A.B. and G.K. performed data analysis and M.A.M.-M., C.M.T. and A.A.B. wrote the manuscript with input from the other authors. All authors reviewed and approved the manuscript.

Competing interests statement

The authors declare no competing non-financial interests.

Figure 1. CRISPR-RfxCas13d system targeting *tbxta* recapitulates no-tail

phenotype in zebrafish embryos. A) Schematic illustration of the experimental set-up used to analyze CRISPR-Cas13 toxicity. 200 pg of mRNA from each Cas13 variant was injected into one-cell stage zebrafish embryos. Cas13b and Cas13d are tagged with HA and Cas13a is fused to GFP. **B)** Toxicity evaluation of embryos. Stacked barplots showing the percentage of deformed and wild type (WT) zebrafish embryos (30 hours post fertilization, hpf) injected in conditions described in **a**. Number of embryos evaluated (n) is shown for each condition. **C)** Schematic of positions of six gRNAs (green lines) targeting *tbxta* CDS in zebrafish (top). Schematic of experimental set-up to analyze CRISPR-RfxCas13d-mediated RNA knockdown in zebrafish (bottom). Two sets of gRNAs targeting *tbxta* CDS (1-3 or 4-6; 300 pg per embryo) were mixed with mRNA (100 or 200 pg per embryo) coding for RfxCas13d (mCas13d) and injected into one-cell stage embryos. **D)** Phenotypic severity in embryos injected with mCas13d and gRNAs targeting *tbxta* (gNTL) compared to uninjected wild type (WT) evaluated at 30 hours post fertilization (hpf) (scale bar, 0.5 mm). Class I: Short tail (least extreme). Class II: Absence of notochord and short tail (medium level). Class III: Absence of notochord and extremely short tail (most extreme). **E)** Different gNTL sets recapitulate *no-tail* phenotype. Stacked barplots showing percentage of observed phenotypes under various injection conditions. Number of embryos evaluated (n) is shown for each condition. **F)** *no-tail* phenotype can be rescued. Stacked barplots showing percentage of observed phenotypes using gNTLs targeting 3'UTR (300 pg/ embryo) and mCas13d (200 pg/embryo) co-injected with different mRNAs: GFP (mGFP CDS, 100 pg/embryo), *tbxta* ORF with 3'UTR from pSP64T plasmid (mNTL CDS, 100 pg/embryo), or *tbxta*

antisense (mNTL anti-se, 100 pg/ embryo) ORF. As an additional control, an unrelated gRNA set targeting a gene involved in germ cell formation (*dnd1*) was included (300 pg/embryo). Number of embryos evaluated (n) is shown for each condition. **G**) qRT-PCR analysis showing levels of *tbxta* mRNA at 7 hours post injection (hpi) in conditions indicated. Results are shown as the averages \pm standard error of the mean from 2 independent experiments with 1 or 2 biological replicates per experiment (n=20 embryos/ biological replicate) for mCas13d alone and Cas13d plus gNTL, respectively. $p=0.0092$ (t-test). *cdk2ap* mRNA was used as normalization control.

Figure 2. CRISPR-RfxCas13d specifically targets reporter mRNAs in zebrafish embryos. Schematics of **A)** *rfp* and *gfp* mRNAs or **B)** *Nano-luciferase* and *Firefly* mRNAs (10 pg/embryo) co-injected with/without mCas13d (200 pg/embryo) and/or gRNAs (250-400 pg/embryo) targeting *rfp* or *Nano-Luciferase* mRNA, respectively. **C)** Fluorescence images of representative embryos at 6 hpi with indicated mRNAs and gRNAs (scale bar, 0.5 mm). **D)** Ratio of nanoluciferase (nano-luc) activity normalized to firefly luciferase activities under indicated conditions at 6 hpi. Results are shown as the averages \pm standard error of the mean from at least 11 biological replicates from two independent experiments (n=5 embryos/ biological replicate). $p < 0.021$, mCas13d and gNANO-LUC compared to other conditions (Kruskal-Wallis test). **E)** qRT-PCR analysis of ratio of RFP reporter mRNAs under indicated conditions at 6 hpi normalized with *gfp* mRNA. Results are shown as the averages \pm standard error of the mean from 2 independent experiments with at least 2 biological replicates per experiment (n=20 embryos/ biological replicate). $p \leq 0.0001$, mCas13d and gRFP compared to other conditions (one-way ANOVA). **F)** Nanoluciferase (nano-luc) mRNA level normalized to firefly mRNA level at 6 hpi at indicated conditions. Results are shown as the averages \pm standard error of the mean from 2 independent experiments with 2 biological replicates per experiment (n=20 embryos/ biological replicate). $p < 0.05$, mCas13d and gNANO-LUC compared to mCas13d alone or mNano-Luc and mFirefly alone (one-way ANOVA). **G)** Schematic of mRNAs (Cas13d and *gfp*) and gRNAs targeting *rfp* introduced into embryos derived from transgenic mother expressing *rfp*. **H)** Fluorescence images of representative embryos at 26 hpi injected with indicated mRNAs and/or gRNAs (scale bar, 0.5 mm). **I)** Scatter plot showing mRNA level (RNA-seq) of zebrafish embryos at 6

hpi. Left panel, mRNA level of uninjected embryos versus embryos injected with mCas13d alone. Right panel, mRNA level of embryos injected with mCas13d plus gRFP versus embryos injected with mCas13d alone. *Rfp* mRNA is indicated in red. Dashed lines indicate a 4-fold difference between RNA levels.

Figure 3. CRISPR-RfxCas13d recapitulates known loss-of-function zebrafish phenotypes.

A) Representative pictures of zebrafish embryos (6 hpi) injected with mCas13d alone or mCas13d plus *szrd1* gRNAs (gSZRD1) (scale bar, 10µm). **B)** Scatter plot showing mRNA level (RNA-seq) of zebrafish embryos injected with mCas13d (250 pg/embryo) alone versus mCas13d plus gSZRD1 (600 pg/embryo) after 6 hpi, *szrd1* mRNA is indicated in red (>7-fold change). Dashed lines indicate a 4-fold difference between RNA levels. **C)** Schematic of mCas13d (200-250 pg/embryo) and *gfp* mRNA containing the 3'UTR of *nanos* (40 pg/embryo) co-injected with/without gRNAs targeting *dnd1* (500-600 pg/embryo) or *tyr* (500-600 pg/embryo). Germ cells are highlighted by germ-cell specific fluorescence (due to *nanos*-3'UTR) at 30 hpf. The ratio of embryos displaying intact germ cells (mCas13d alone or mCas13d plus gTYR) or without germ cells (mCas13d plus gDND1) vs total number of analyzed embryos (at least from two independent experiments) are indicated (scale bar, 0.5 mm). **D)** Scatter plot showing mRNA level (RNA-seq) of zebrafish embryos injected with mCas13d (250 pg/embryo) alone versus mCas13d plus *dnd1* gRNAs (600 pg/embryo) after 6 hpi, *dnd1* mRNA is indicated in red (~8-fold change). Dashed lines indicate a 4-fold difference between RNA levels. **E)** Representative pictures of epiboly-stage zebrafish embryos displaying gastrulation and epiboly defects in embryos injected with mCas13d plus *nanog* gRNAs (gNANOG), but not in embryos injected with either mCas13d alone or mCas13d plus *gfp* gRNAs (gGFP). The ratios of embryos displaying normal development (mCas13d mRNA alone or mCas13d mRNA plus gGFP) or with epiboly and gastrulation defects (mCas13d mRNA plus gNANOG) vs total number of analyzed embryos are indicated.

Embryos were injected with 250 pg, 430 pg and 600 pg of mCas13d, gGFP and gNANOG, respectively (scale bar, 0.1 mm). **F)** Scatter plot showing mRNA level (RNA-seq) of zebrafish embryos injected with mCas13d plus gNANOG compared to embryos injected with mCas13d alone at 6 hpi. *nanog* mRNA is indicated in red. Black outline indicates genes that display reduced expression (>4-fold decrease) in *nanog* morpholino-treated (MO) embryos. Dashed lines indicate a 4-fold difference between RNA levels. **G)** Representative pictures of zebrafish embryos injected with mCas13d plus the indicated gRNAs targeting *smad5*, *alk8*, *oep* and *smad2* mRNA showing the recapitulated phenotypes. **H)** Pigmentation phenotypes (52 hpf) of head/eyes of embryos injected with mCas13d alone (300 pg/embryo, left), *tyr* gRNAs alone (600 pg/embryo, center), or both (right) (scale bars, 0.5 mm). The ratios of embryos displaying intact pigmentation (mCas13d or gTYR alone) or with the lack of pigmentation (mCas13d plus gTYR) vs total number of analyzed embryos are indicated.

Figure 4. RfxCas13d protein enhances maternal RNA targeting.

A) Schematic illustration of the experimental set-up to use CRISPR-Cas13d purified protein. **B)** Stacked barplots showing percentage of observed phenotypes in embryos injected with *RfxCas13d* mRNA (mCas13d) or protein (Cas13d Prot.), alone or together with *in vitro* transcribed (gNANOG) or chemically synthesized (gNANOG-Synt) gRNAs. The amount of gRNA, mRNA or protein injected per embryo is indicated. Number of embryos evaluated (n) is shown for each condition. Representative pictures of epiboly-stage zebrafish embryos displaying gastrulation and epiboly defects in embryos injected with Cas13d protein plus gNANOG are shown in the top panel. 30% epiboly, 50% epiboly, germ ring and shield stages correspond to 4.6, 5.3, 5.7, and 6 hpf in wild type embryos growing in standard conditions, respectively (scale bar, 0.5 mm). **C)** qRT-PCR analysis of *nanog* mRNA in embryos at 2 and 4 hpi injected with mCas13d or protein alone or together with gRNAs targeting *nanog* mRNA. Results are shown as the averages \pm standard error of the mean from 2 independent experiments with at least 2 biological replicates per experiment (n=10 embryos/biological replicate). *Taf15* mRNA was used as normalization control. ($p < 0.05$, $** < 0.01$, $*** < 0.001$ t-test, comparing each knock-down condition vs its corresponding control). **D)** Fluorescence pictures of zebrafish embryos (30 hpi) injected with Cas13d protein (3ng) and GFP with *nanos* 3'UTR (40 pg) without or with gDND1 (400pg). Insets show magnification of the region where the germ line forms. The ratio of embryos displaying intact germ cells (mCas13d alone) or without germ cells (mCas13d plus gDND1) vs total number of analyzed embryos (at least from two independent experiments) are indicated (scale bar, 0.5 mm). **E)** Representative pictures of zebrafish embryos (7 hpi) injected with Cas13d protein

alone (3ng) or Cas13d protein plus gSZRD1s (400pg) (scale bar, 10 μ m). **F)** Scatter plot showing mRNA level (RNA-seq) of zebrafish embryos injected with Cas13d protein plus *dnd1* or *szrd1* gRNAs compared to embryos injected with Cas13d protein alone at 6 hpi. *Dnd1* and *szrd1* mRNAs are indicated in red in their respective panels (>7-fold and >6.3-fold decrease, respectively). Dashed lines indicate a 4-fold difference between RNA levels. **G)** qRT-PCR analysis showing levels of *brd3a*, *brd3b* and *brd4* mRNAs in embryos at 4 hpi injected with Cas13d protein alone (3 ng/embryo) or together with gRNAs (300 pg/embryo) targeting the different *brds* mRNAs. Results are shown as the averages \pm standard error of the mean from 2 independent experiments with at least 2 biological replicates per experiment (n=10 embryos/biological replicate). Taf15 mRNA was used as normalization control ($p^* < 0.05$, $** < 0.01$, t-test comparing each knock-down condition vs its corresponding control). **H)** Stacked barplots showing percentage of observed phenotypes using gRNAs targeting *brd3a*, *brd3b* and *brd4* mRNAs co-injected with Cas13d protein at the same concentrations. Number of embryos evaluated (n) is shown for each condition. The phenotype selection criteria were the same as in panel **B**.

Figure 5. CRISPR-RfxCas13d as RNA targeting tool in different animal models.

A) Representative pictures of medaka embryos at 68 hpf showing arrested eye development in embryos injected with mCas13d (450 pg) with gRNAs (1 ng) targeting *rx3* mRNA (gRX3) compared to the embryos injected with mCas13d alone or uninjected embryos. Double arrows and asterisk indicate eye length and absence of eye, respectively (scale bar, 0.1mm). **B)** Fluorescence microscopy images of killifish embryos showing RFP and GFP intensity of uninjected embryos or after 14 hpi injected with *rfp* and *gfp* mRNAs, with or without mCas13d (250-350 pg/embryo) and/or gRNAs (300 – 400 pg/embryo) targeting *rfp* mRNA (scale bar, 0.1 mm). **C)** Fluorescence microscopy images of mouse embryos 24 hours post injection (2 cell-stage) with *rfp* and *gfp* mRNAs with or without mCas13d and/or gRNAs targeting *rfp* or unrelated (zebrafish *tyr*) mRNA (scale bar, 100 um). **D)** Stacked plots showing the percentage of mouse embryos at 2 or 4 cells stage 48 hours post injection with the indicated mRNA and/or gRNAs. The number of embryos (n) is indicated from at least two independent experiments.

Star Methods

Resource Availability:

Lead Contact:

Further information and requests for resources and reagents should be directed to and will be fulfilled by the Lead Contact, Miguel A. Moreno-Mateos (mamormat@upo.es).

Materials Availability:

Key plasmids generated in this study are available in addgene (#141320 ,#141321 and #141322).

Data and Code availability:

Original data (from Stowers and CABD) underlying this manuscript can be accessed from the Stowers Original Data Repository at <http://www.stowers.org/research/publications/libpb-1454>. The Stowers Institute contributing authors have selected to present the raw data of this manuscript resulting from work performed at The Stowers Institute. The RNA-seq data have been deposited in GEO under accession code GSE135884. All the mRNA level measures by RNA-seq are provided in Table S2. All other relevant data are available from corresponding authors upon reasonable request.

Experimental model and subject details

Zebrafish maintenance and embryo production

All experiments involving zebrafish at CABD conform national and European Community standards for the use of animals in experimentation and were approved by the Ethical committees from the University Pablo de Olavide, CSIC and the Andalucian Government. Zebrafish wild type strains AB/Tübingen (AB/Tu) were maintained and

bred under standard conditions (Westerfield, 1995). Wild-type zebrafish embryos were obtained through natural mating of AB/Tu zebrafish of mixed ages (5–18 months). Selection of mating pairs was random from a pool of 20 males and 20 females. Zebrafish embryos were staged in hours post-fertilization (hpf) as described (Kimmel et al., 1995). Zebrafish experiments at Stowers Institute were done according to the IACUC approved guidelines. Zebrafish embryos collected for microinjections were coming from random parents (AB, TF and TLF, 6-25 months old) mating from 4 independent strains of a colony of 500 fish. The embryos were pooled from random 24 males and 24 females for each set of experiment. Wild type fish lines from University of New Haven were maintained in accordance with OLAW and USDA research guidelines, under a protocol approved by the University of New Haven IACUC. Twenty couples of males and females (TU and AB intermixed strains, 6-18 month old) were randomly selected and crossed to generate embryos for experiments described herein. For each set of experiments from different laboratories both controlled and test embryos after injections were kept in similar condition and 100-800 embryos were injected per experiment (depending on the need of the experiment).

Embryos for the PrP-1 experiments were obtained from single, 12 month old fish couples belonging to the Tab5 strain (Tü and AB hybrid) at UPCH in Lima. Adult fish were kept at the UPCH animal facility following standard procedures (Westerfield, 1995) and research guidelines approved by the University IACUC. Embryos were raised and staged as previously described (Kimmel et al., 1995).

Medaka maintenance and embryo production

All experiments involving medaka conform national and European Community standards for the use of animals in experimentation and were approved by the Ethical committees from the University Pablo de Olavide, CSIC and the Andalucian Government. The medaka wild type strain (iCab) was maintained and bred under standard conditions. 15-20 couples of males and females (4 months old) were randomly selected and crossed to generate embryos for experiments described herein. Embryos were injected at single cell stage also according to standard procedures (Kinoshita et al., 2012). Embryos were staged in hours post-fertilization (hpf) as described (Iwamatsu, 2004).

Killifish maintenance and embryo production

All experiments involving killifish at Stowers Institute were done according to the IACUC approved guidelines (2019-090). Random 3-to-4 months old individuals of killifish strain- inbred GRZ line, with opposite sex were crossed and embryos were pooled for each set of experiment. Three breeding tanks were used for embryos collection. Each tank contained one single male and 5 female.

Mouse maintenance and embryo donors

Immature C57BL/6J female mice (3-4 weeks of age) were utilized as embryo donors. The C57BL/6J females were super ovulated following standard procedures with 5 IU PMSG (Genway Biotech #GWB-2AE30A) followed 46 hours later with 5 IU hCG (Sigma #CG5) and subsequently mated to fertile C57BL/6J stud males (4-6 months of age). Females were checked for the presence of a copulatory plug the following morning as an indication of successful mating. Out of the 20 super-ovulated females, approximately 10 – 12 females were plugged and harvested for embryo microinjection

for each set of experiment. One-cell fertilized embryos were collected from the oviducts of mated females at 0.5 days post coitus and placed in KSOM media in a CO₂ incubator at 37° C, 5% CO₂ until microinjection. Animals were maintained in Lab Animal Service Facility (LASF) of Stowers Institute at 14:10 light cycle and provided with food and water *ad libitum*. Experimental protocols were approved by the Institutional Animal Care and Use Committee at Stowers Institute and were in compliance with the NIH Guide for Care and Use of Animals.

Method details

Guide RNA and mRNA generation

For a more detailed protocol please see the extended protocol, Methods S1. Guide RNA (gRNA) design was based on CRISPR-Cas13 targeting data in mammalian cell culture in which there was not any significant protospacer flanking site preference (PFS) reported and gRNA activity partially correlated with target accessibility (Abudayyeh et al., 2017; Konermann et al., 2018). Thus, full mRNA targets or 70 nt long sliding windows of the mRNA were analyzed *in silico* using RNAfold software (<http://rna.tbi.univie.ac.at/cgi-bin/RNAWebSuite/RNAfold.cgi>) (Lorenz et al., 2011) and protospacers of 22 nucleotides (target sequences) with high accessibility (low base-pairing probability from minimum free energy predictions) within the target mRNAs were selected to generate gRNAs. DNA template to generate gRNA was generated by fill-in PCR (Figures S1E and S1F). A gRNA universal primer (Table S1) containing the T7 promoter (5'-TAATACGACTCACTATA-3') and the processed direct repeat for Cas13d gRNAs (30 nt) preceded by 5'GG was used in combination with a specific oligo of 42 nt adding the spacer (22 nt for target-binding) and part of the repeat sequence (reverse

complement orientation). A 71 (bp PCR product was generated following these conditions: 3 min at 95°C, 35 cycles of 30s at 95°C, 30s at 51°C, and 30s at 72°C, and a final step at 72 °C for 7 min. PCR products were purified using Favorprep Gel/PCR purification kit (Favorgen) columns or PCR purification kit (ThermoFisher) and used as template (400-900 ng) for a T7 in vitro transcription reaction (AmpliScribe-T7-Flash transcription kit from Epicenter; 12-16 h of reaction). *In vitro* transcribed gRNAs were DNase-treated using TURBO-DNase for 15 min at 37°C and precipitated with Sodium Acetate/Ethanol. gRNAs were visualized in a 2% agarose stained by ethidium bromide to check for RNA integrity and quantify using Qubit™ RNA BR Assay Kit (ThermoFisher, Q10210). gRNAs targeting *tbxta*, *brd3a*, *brd3b*, *brd4* and *tyr* CDS in zebrafish and *rx3* in medaka were *in vitro* transcribed from PCR containing a pool of different gRNA primers at equal concentration. All other gRNAs were individually *in vitro* transcribed and mix at equal concentrations in pools after the *in vitro* transcription. To increase mRNA depletion 3-4 gRNAs targeting the same mRNA were co-injected, otherwise is specified in figure legends. Solid-phase extraction-purified gRNAs targeting *nanog* and *tbxta* mRNAs were generated by Synthego.

Human codon-optimized Cas13d or NLS-Cas13d-NLS were PCR-amplified using primers Rfx13d_Fw and Rfx13d_Rv and Rfx13d-NLS_Fw and Rfx13d-NLS_Rv, respectively (Table S1) and using addgene plasmid # 109049 (a gift from Patrick Hsu) as template (Konermann et al., 2018). The following PCR products were then digested with *NcoI* and *SacII* and ligated into the pT3TS-nCas9n (Jao et al., 2013) plasmid previously digested with the same enzymes to generate pT3TS-RfxCas13d and pT3TS-RfxCas13d-NLS (addgene # 141320 and 141321, respectively). pT3TS-RfxCas13d was

cut with *NcoI* and *NotI* and RfxCas13d without HA was cloned into pET-28b cut with similar restriction enzymes generating pET-28b-RfxCas13d-HIS (addgene # 141322). Human codon-optimized PspCas13b and PguCas13b inserts were PCR-amplified from addgene plasmids #103862 and #103861 (a gift from Feng Zhang) (Cox et al., 2017) using primers PspCas13b_FW/RV (Table S1) and PguCas13b_FW/FR, respectively (Table S1). Both Cas13 PCR amplicons were subsequently digested using *EcoRI*- and *NotI*, then were cloned into vector pSP64T (Moreno-Mateos et al., 2017), which was previously digested with the same restriction enzymes. LwaCas13a-msfGFP, without and with NLS, was amplified from addgene plasmid #91902 (a gift from Feng Zhang) using primers Cas13aORF_Fw and Cas13aORF_Rv or Cas13aORF-NLS_Rv (Table S1), respectively. Both Cas13 PCR amplicons were subsequently digested using *EcoRI*- and *XhoI*, then were cloned into vector pSP64T. *tbxta* ORF (sense and antisense) was PCR amplified (Table S1). PCR products were digested with *EcoRI* and cloned into pSP64T previously digested with the same enzyme. p515-Tol2-attP-Ubi-RFP expression vector (see below RFP transgenic zebrafish section) was built by first cloning tag-RFP from p514-Ubi-TagRFP (a gift from Daniel Cifuentes of Boston University School of Medicine) into p328-attB-ubi:EGFP (Mosimann et al., 2011) via NEBuilder HiFi assembly kit (NEB) using PCR products from p328 plasmid amplified with pDest-gibson_FW/RV primers (Table S1) and from p514 plasmid amplified with tagRFP-Ubi_FW/RV (Table S1). Next the subsequent construct was digested using *KpnI* and *NotI*. Plasmid p511-Tol2-attP-Tol2, purchased from GENEWIZ (Kwan et al., 2007), was digested using the same enzymes and cloned into the p328 digest, resulting in the final expression plasmid used for transgenesis, p515-Tol2-attP-Ubi-RFP. All final

constructs were confirmed by Sanger sequencing (Data S1).

To generate *tbxta*, *RfxCas13d* mRNA and *LwaCas13a-GFP* the DNA templates were linearized using *XbaI* and with *SmaI*, *SacI* to produce *PspCas13b*, *PguCas13b*, respectively. mRNA was synthesized using the mMachine T3 (*Cas13d*) or SP6 (*Cas13b*, *tbxta* and *Cas13a*) kit (Ambion). *In vitro* transcribed mRNAs were DNase-treated using TURBO-DNase for 15 min at 37°C and purified using the RNeasy Mini Kit (Qiagen) and quantified using Qubit™ RNA BR Assay Kit (ThermoFisher, Q10210).

Sample preparation and Western blot

Ten embryos were collected at 6 hours post injection and washed twice with 200 µL of deysolking buffer (55 mM NaCl, 1.8 mM KCl, and 1.25 mM NaHCO₃). Then, samples were incubated for 5 min with orbital shaking and centrifuged at 300 g for 30 s. Supernatant was removed and embryos were washed with 110 mM NaCl, 3.5 mM KCl, 10 mM Tris-HCl pH 7.4, and 2.7 mM CaCl₂. Finally, embryos were centrifuged again and the supernatant was removed. The pellet was resuspended in SDS-PAGE sample buffer (160 mM Tris-HCl pH 8, 20% Glycerol, 2% SDS, 0.1% bromophenol blue, 200 mM DTT).

Sample separation by SDS-PAGE electrophoresis was performed using 10% TGX Stain-Free™ Fast Cast™ Acrylamide Solutions (Bio-Rad). After electrophoresis, protein gels were activated in a Chemidoc MP (Bio-Rad) and blotted to Nitrocellulose membranes using the Trans-Blot Turbo Transfer System (Bio Rad). Membrane was blocked for 1 h at room temperature in Blocking Solution (5% fat free milk in 50 mM Tris-Cl, pH 7.5, 150 mM NaCl (TBS) with 1% Tween20). Primary antibody Anti-HA (11867423001, Roche) and secondary antibody anti-mouse HRP-labelled (A5278,

Sigma-Aldrich) were diluted 1:1000 and 1:10.000 respectively in Blocking Solution. Membrane was incubated in primary antibody o/n at 4°C. After primary antibody incubation membrane was washed three times briefly with TBS with 1% Tween 20 (TTBS) for 10 min and incubated with the secondary antibody for 60 min at room temperature. Washes were performed as with primary antibody. The detection was done with Clarity™ Western ECL Substrate (Bio-Rad) and images were acquired using a ChemiDoc MP (Bio-Rad). Chemiluminiscent signal was normalized using ImageLab software (Bio-Rad) with Stain Free total lane volumes (Gurtler et al., 2013).

Expression and purification of RfxCas13d

The pET28B-RfxCas13d-His plasmid containing the recombinant Cas13d protein was chemically transformed into *Escherichia coli* Rosetta™ (DE3) competent cells (Novagen). Cells were grown at 37°C until OD600 0.5 and induced with 0.1 mM IPTG during 3 h. Cells were then pelleted, washed with 20 mM Tris-HCl pH 7.6 and frozen until use at -80°C.

For protein purification, induced cell pellet was resuspended in lysis buffer (50 mM HEPES·KOH pH 7.5, 500 mM KCl, 10% v/v glycerol, 1mM DTT and 10 mM imidazole) and sonicated in a Branson SFX550 sonifier with 5 s on-10 s off cycles during 10 minutes at 40% amplitude on ice. Lysate was clarified by centrifugation at 8.000 g for 10 min at 4°C and filtered with 0.2 µm Cellulose acetate filters. Cas13d-His protein was purified using a HisTrap FF column (GE Healthcare) connected to a Äkta Pure System (GE Healthcare). After sample application, column was washed with 20 CV of lysis buffer and the protein was dissociated from the column with a two-step elution protocol: first with 5 CV of 10% Elution buffer (50 mM HEPES·KOH pH 7.5, 500

mM KCl, 10% v/v glycerol, 1mM DTT and 500 mM imidazole) and second with of 20 CV gradient until 50% of Elution buffer is reached. Fractions containing purified recombinant protein (Fig S4A) were pooled, dialyzed at 4°C overnight against dialysis buffer (50 mM HEPES·KOH pH 7.5, 250 mM KCl, 1 mM DTT and 10% glycerol) and concentrated by ultrafiltration with a 30K Amicon Ultra-15 (Merck, Millipore) at 4°C until reach a concentration of 3 µg/µL. Protein concentration was calculated using the RC-DC™ Protein Assay kit (Bio-Rad) and protein purity was analysed by densitometry. Aliquots with 5 µL of Cas13d were stored at –80 °C.

Zebrafish embryo injection and image acquisition

1-2 nL containing 100-300 pg of *cas13(s)* mRNA or 1.5-3 ng of purified Cas13d protein and 300-1000 pg of gRNA were injected in the cell of one-cell stage embryos (see figure legends for details in each experiment). Cas13d protein and gRNAs were injected in two rounds to maximize the amount of protein and gRNA (at the indicated concentrations) per injection. Alternatively RNPs were assembled in dialysis buffer by mixing Cas13d and gRNAs and co-injected in one round. Morpholino Prp-1 injection was carried out as described in Sempou et al. (Sempou et al., 2016). Phenotypes and samples were collected, analyzed and quantified between 2 hours and 5 days post injection depending on the experiment. Zebrafish embryo phenotypes and fluorescent pictures were analysed using an Olympus SZX16 stereoscope and photographed with a Nikon DS-F13 digital camera and images processed with NIS-Elements D 4.60.00 software or were imaged using Zeiss SteREO Lumar.V12 and Leica MZ APO stereomicroscopes. Ppr-1 scoring of morphological phenotypes was done under an Axiozoom v16 stereoscope (Zeiss). Images were captured using the ZEN software

(Zeiss) and further edited in Adobe Photoshop. GFP and RFP fluorescence were quantified using Fiji (Image J) software. GFP and RFP fluorescence was subtracted to uninjected embryos and then final values calculated.

Transgenic RFP zebrafish:

Transgenic zebrafish were kept according to the National Research Council's and IACUC approved protocol 2016-1059 at the Stowers Institute for Medical Research zebrafish facility. Wild-type embryos obtained from breeding of adult AB-TU and TL-TLF strains were co-injected with 1 nL p515-Tol2-attP-Ubi-RFP (20 ng/ul) and capped transposase mRNA (50 ng/ul) (Kwan et al., 2007), at one-cell stage. Mosaic larvae demonstrating positive RFP fluorescence at 5 days post fertilization (dpf) were raised to 70 dpf and outcrossed to TL-TLF wild-type fish. These embryos were screened at 5 dpf for ubiquitous RFP fluorescence and positive individuals were raised to use for embryo production. F2 embryos coming from RFP positive mothers were injected with mCas13d and RFP gRNAs.

***In situ* hybridization (ISH) and *shh* RNA Probe Synthesis**

ISH was performed using digoxigenin-labeled antisense RNA probes following (Thisse and Thisse, 2008) with the following changes. During wash steps and incubation steps, embryos were placed in 1.5 mL tubes in place of 6 and 24 well plates. Solutions were added and removed from the tube using a pasteur pipette instead of transferring embryos to solution using small/large baskets as described in the protocol. Washes and incubations were performed without the use of a horizontal shaker.

To generate *shh* in situ probe RNA was extracted from 25 zebrafish embryos at 24 hpf using TRIzol reagent (ThermoFisher Scientific). cDNA was synthesized using SuperScript™ III First-Strand Synthesis System. *shh* was amplified by PCR using the following primers. Forward: 5'ATGCGGCTTTTGACGAGAGTGCTG3'. Reverse: 5'TAATACGACTCACTATAGGGTCAGCTTGAGTTTACTGACA TC3'. Primers were designed to amplify the full 1257bp *shh* coding sequence. The reverse primer contained a T7 promoter, which allowed for antisense *shh* probe synthesis using T7 RNA polymerase. Probe synthesis was carried out following (Thisse and Thisse, 2008).

RNA-seq libraries and analysis:

mRNAseq libraries were generated from 500 ng of high-quality total RNA, as assessed using the Bioanalyzer (Agilent). Libraries were made according to the manufacturer's directions for the TruSeq Stranded mRNA LP Sample Prep Kit (Illumina, Cat. No. 20020594) with TruSeq RNA Single Indexes Set A and B (Illumina, Cat. No. 20020492 and 20020493). Resulting short fragment libraries were checked for quality and quantity using the Bioanalyzer (Agilent) and Qubit Fluorometer (Life Technologies). Libraries were pooled, re-quantified and sequenced as 75bp single reads on a high-output flowcell using the Illumina NextSeq instrument. Following sequencing, Illumina Primary Analysis version RTA 2.4.11 and bcl2fastq2 v2.18 were run to demultiplex reads for all libraries and generate FASTQ files.

RNA-seq reads were aligned using STAR version 2.6.1c to *Danio rerio* reference genome danRer11 from University of California at Santa Cruz with RFP exogenous sequence incorporated in its index. Transcripts were quantified using RSEM version 1.3.0 to calculate the transcript abundance 'TPM' (Transcript per Million). Fold change

for each gene was calculated using edgeR version 3.24.3 after filtering genes with a count of 10 reads in at least one library. The resulting p values were adjusted with Benjamini-Hochberg method using R function `p.adjust`. Genes with less than 6.5 TPMs in the embryos injected with Cas13d alone were filtered. To define potential off-targets, each gRNA was aligned to the longest transcript of all genes in danRer11 using EMBOSS Water (Smith and Waterman, 1981) wrapper from Biopython. The sum of base changes and gaps in the alignment were considered as the mismatch score of the gRNA. The minimum mismatch score of all the gRNA's in each targeted gene was taken and genes with minimum mismatch score < 4 are shown in the plot.

qRT-PCR

For checking the level of targeted mRNA in zebrafish embryos, 20 embryos per biological replicate were collected for all except Figure 4 (see below) zebrafish qRT-PCRs at the described hours post injection in figures or legends and snap frozen in liquid nitrogen. Total RNA was isolated using standard TRIzol protocol as described in the manual (ThermoFisher Scientific). The cDNA was synthesized using SuperScript™ IV First- Strand Synthesis System, following the manufacturer's protocol. To set up the real time qPCR for different genes, 1/25 cDNA dilution was used using forward and reverse primers per mRNA (10 μ M; Table S1) in a 10 μ L reaction. Samples were prepared as instructed for automated Freedom EVO® PCR workstation (Tecan) and run in QuantStudio 7 Flex Thermo cycler (Applied Biosystem). For Figure S3L, for each mRNA targeted, the embryos injected with Cas13d with the unrelated gRNAs were used as control. For figure 4 qRT-PCR, 10 embryos per biological replicate were collected at the 2 or 4 hpf, snap frozen in liquid nitrogen. Total RNA was obtained as described

above and 1000 ng of purified total RNA was then reverse transcribed using the iScript cDNA synthesis kit (Bio-Rad), following the manufacturer's protocol. 2 µl from a 1/5 dilution of the cDNA reaction was used in a 10 µl reaction containing 1.5 µl of forward and reverse primers (2 µM each; Table S1), 5 µl of iTaq Universal SYBR Green Supermix (Bio-Rad) and run in a CFX connect instrument (Bio-Rad). PCR cycling profile consisted in a denaturing step at 95 °C for 30 s and 40 cycles at 95 °C for 10 s and 60 °C for 30 s (*mxtx2*, *klf17*, *vgl14l*) or 40 cycles at 95 °C for 10 s, 58 °C for 10 s and 30 s at 72 °C (*brd3a*, *brd3b*, *brd4*). As controls *cdk2ap2* or *taf15* mRNAs were used since their levels do not change during the first 6 hours of zebrafish development in standard conditions (Bazzini et al., 2016).

Eight medaka embryos were collected at stage 16 (21 hpf) per biological replicate (except for WT uninjected that 5 embryos were collected). Total RNA was isolated from embryos injected using TRIzol reagent (ThermoFisher Scientific). An amount of 500-1000 ng of purified total RNA was then subjected to reverse transcription using the iScript cDNA synthesis kit (Bio-Rad), following the manufacturer's protocol. 4.5 microliters from a 1/25 dilution of the cDNA reaction was used to determine the levels of *rx3* mRNA in a 10 µL reaction containing 0.5 µL of forward and reverse primers (10 µM each; Table S1), using iTaq Universal SYBR Green Supermix (Bio-Rad) and a CFX connect instrument (Bio-Rad). PCR cycling profile consisted in a denaturing step at 95 °C for 30 s and 40 cycles at 95 °C for 10 s and 60 °C for 30 s. Two technical qPCR replicates were performed per biological replicate.

Nano-luciferase activity:

For nano-luciferase mRNA targeting, 10 pg of nano-luciferase mRNA and firefly luciferase mRNA (as an internal control) together with different experimental conditions including mCas13d (200 pg) and/or gRNA-nanoluciferase cocktail (400 pg) were injected per zebrafish embryo at one cell stage. Injected embryos were collected at 6 hours post injection and at least 8 tubes (5 embryos per tube) per condition were snap frozen in liquid nitrogen. Nano-Glo Dual-Luciferase® reporter assay protocol (Promega) was followed as instructed in the manual for assaying the activity of nanoluciferase and firefly luciferase activity using infinite M200 PRO by TECAN. To have comparable samples, those with more than 2 fold firefly activity in comparison to the uninjected control average (nano-luciferase and firefly luciferase mRNAs only) were not included in the analysis.

Medaka embryo injection and image acquisition (phenotypes)

2 nL containing 450 pg of mCas13d and 1 ng of gRNA were injected in one-cell stage embryos. Embryos phenotype was examined and photographed between 30 and 72 hpf using a stereoscope (SZX16–DP71, Olympus).

Killifish Microinjection and image acquisition

Approximately 200 killifish embryos were injected at single cell stage with ~2 nl containing 200 pg of mCas13d and 600 pg of gRNA. Embryos were held in 1 mm-wide trenches on a 1.5% agarose plate during injection. Embryos were kept in 1X Yamamoto's embryo solution with 0.0001% methylene blue at 28° Celsius in the darkness and fluorescent pictures were imaged using Leica M205 FCA stereomicroscopes. GFP and RFP fluorescence from these images were

quantified using Fiji (Image J) software. GFP and RFP fluorescence was subtracted to uninjected embryos and then final values calculated.

Mouse embryo injections and image acquisition

CRISPR-RfxCas13d reagents were microinjected into both the pronucleus and cytoplasm (1-2 pl total) of one-cell embryos using previously described techniques (Nagi et al., 2003). In brief, microinjection was performed using a Nikon Eclipse Ti inverted microscope equipped with Eppendorf TansferMan micromanipulators, Eppendorf CellTram Air® for holding of embryos, and Eppendorf FemtoJet® auto-injector. A small drop of M2 media was placed on a siliconized depression slide and approximately 20-30 C57BL/6J oocytes were transferred to the slide for microinjection. The slide was placed on the stage of the microscope and oocytes were injected at 20x. Immediately following microinjection, the embryos were returned to the CO2 incubator in KSOM culture media and observed daily for embryo development.

For toxicity testing, embryos were injected as described above with varying concentrations of mCas13d to test for toxicity. Injections concentrations were 2.5 ng/ul, 10 ng/ul, 25 ng/ul and 50ng/ul. A Stock solution of mCas13d was serially diluted using Tris Low EDTA microinjection buffer. Initial observations indicated the embryos responded normally to the microinjection. Embryos were cultured overnight as described above and observed the following morning for development. Embryos were returned to the incubator and observed each day to track the development to the 3.5 days post coitus blastocyst stage.

For mCas13d and gRNA Injections, reagents were prepared and delivered on ice at the desired injection concentrations. Injections concentrations were mCas13d (25

ng/ul), gRNA RFP (100 ng/ul), *GFP* and *RFP* mRNA (8-10 ng/ul). Fluorescent images were taken using Nikon ECLIPSE Ti 2 microscope. GFP and RFP fluorescence from these images were quantified using Fiji (Image J) software. GFP and RFP fluorescence was subtracted to uninjected embryos and then final values calculated.

Quantification and statistical analysis

No statistical methods were used to predetermine sample size. The experiments were not randomized, and investigators were not blinded to allocation during experiments and outcome assessment. No data were excluded from the analysis unless is specified in other methods section. Unpaired two-tailed Mann–Whitney test was used to compare the results from CRISPR-RfxCas13d and Morpholino (MO) targeting *nanog*. Toxicity and phenotype data in different injections conditions (*tbxta*, *nanog*, *brd*) come from, at least, two independent experiments per figure panel and χ^2 -test (Chi-squared) test was used to analyze significance. These tests were performed using R. For early embryo viability, quantitative RT-PCR, RIN index, RFP/GFP intensity and luciferase activity *p* value was calculated using unpaired t-test, one-way ANOVA test or Kruskal-Wallis test using Prism (GraphPad Software, La Jolla, CA, USA) and Standard Error of the Mean (SEM) was used to show error bars (otherwise is specified in figure legends). As it was described in the RNA-seq section, the fold change for each gene was calculated using edgeR version 3.24.3 after filtering genes with a count of 10 reads in at least one library. The resulting *p* values were adjusted with Benjamini-Hochberg method using R function *p* value adjusted using two biological replicates.

Supplemental video and table titles

Table S1. Oligonucleotides, gRNAs and endogenous mRNA IDs used in this study, Related to Figure 1-5.

Table S2. mRNA levels by RNA-seq in this study, Related to Figure 2-4.

Data S1. Nucleotide sequence of all the vectors used in this study, Related to Figure 1-5.

Methods S1. Extended protocol describing each step to generate gRNAs and RfxCas13d and procedures to inject them into zebrafish embryos, Related to Figure 1-5

References

- Abrams, E.W., and Mullins, M.C. (2009). Early zebrafish development: it's in the maternal genes. *Current opinion in genetics & development* 19, 396-403.
- Abudayyeh, O.O., Gootenberg, J.S., Essletzbichler, P., Han, S., Joung, J., Belanto, J.J., Verdine, V., Cox, D.B.T., Kellner, M.J., Regev, A., *et al.* (2017). RNA targeting with CRISPR-Cas13. *Nature* 550, 280-284.
- Abudayyeh, O.O., Gootenberg, J.S., Konermann, S., Joung, J., Slaymaker, I.M., Cox, D.B., Shmakov, S., Makarova, K.S., Semenova, E., Minakhin, L., *et al.* (2016). C2c2 is a single-component programmable RNA-guided RNA-targeting CRISPR effector. *Science* 353, aaf5573.
- Aman, R., Ali, Z., Butt, H., Mahas, A., Aljedaani, F., Khan, M.Z., Ding, S., and Mahfouz, M. (2018). RNA virus interference via CRISPR/Cas13a system in plants. *Genome biology* 19, 1.
- Bauer, H., Lele, Z., Rauch, G.J., Geisler, R., and Hammerschmidt, M. (2001). The type I serine/threonine kinase receptor Alk8/Lost-a-fin is required for Bmp2b/7 signal transduction during dorsoventral patterning of the zebrafish embryo. *Development* 128, 849-858.
- Bazzini, A.A., Del Viso, F., Moreno-Mateos, M.A., Johnstone, T.G., Vejnar, C.E., Qin, Y., Yao, J., Khokha, M.K., and Giraldez, A.J. (2016). Codon identity regulates mRNA stability and translation efficiency during the maternal-to-zygotic transition. *The EMBO journal* 35, 2087-2103.
- Bazzini, A.A., Johnstone, T.G., Christiano, R., Mackowiak, S.D., Obermayer, B., Fleming, E.S., Vejnar, C.E., Lee, M.T., Rajewsky, N., Walther, T.C., *et al.* (2014). Identification of small ORFs in vertebrates using ribosome footprinting and evolutionary conservation. *The EMBO journal* 33, 981-993.
- Bellipanni, G., Varga, M., Maegawa, S., Imai, Y., Kelly, C., Myers, A.P., Chu, F., Talbot, W.S., and Weinberg, E.S. (2006). Essential and opposing roles of zebrafish beta-catenins in the formation of dorsal axial structures and neurectoderm. *Development* 133, 1299-1309.
- Buchman, A., Brogan, D.J., Sun, R., Yang, T., Hsu, P., and Akbari, O. (2020). Programmable RNA Targeting using CasRx in Flies. *bioRxiv*.
- Camp, E., and Lardelli, M. (2001). Tyrosinase gene expression in zebrafish embryos. *Development genes and evolution* 211, 150-153.
- Chan, S.H., Tang, Y., Miao, L., Darwich-Codore, H., Vejnar, C.E., Beaudoin, J.D., Musaev, D., Fernandez, J.P., Benitez, M.D.J., Bazzini, A.A., *et al.* (2019). Brd4 and P300 Confer Transcriptional Competency during Zygotic Genome Activation. *Developmental cell* 49, 867-881 e868.
- Chen, G.R., Sive, H., and Bartel, D.P. (2017). A Seed Mismatch Enhances Argonaute2-Catalyzed Cleavage and Partially Rescues Severely Impaired Cleavage Found in Fish. *Molecular cell* 68, 1095-1107 e1095.
- Ciruna, B., Weidinger, G., Knaut, H., Thisse, B., Thisse, C., Raz, E., and Schier, A.F. (2002). Production of maternal-zygotic mutant zebrafish by germ-line replacement. *Proceedings of the National Academy of Sciences of the United States of America* 99, 14919-14924.

Cox, D.B.T., Gootenberg, J.S., Abudayyeh, O.O., Franklin, B., Kellner, M.J., Joung, J., and Zhang, F. (2017). RNA editing with CRISPR-Cas13. *Science* 358, 1019-1027.

Dubrulle, J., Jordan, B.M., Akhmetova, L., Farrell, J.A., Kim, S.H., Solnica-Krezel, L., and Schier, A.F. (2015). Response to Nodal morphogen gradient is determined by the kinetics of target gene induction. *eLife* 4.

El-Brolosy, M.A., Kontarakis, Z., Rossi, A., Kuenne, C., Gunther, S., Fukuda, N., Kikhi, K., Boezio, G.L.M., Takacs, C.M., Lai, S.L., *et al.* (2019). Genetic compensation triggered by mutant mRNA degradation. *Nature* 568, 193-197.

Freije, C.A., Myhrvold, C., Boehm, C.K., Lin, A.E., Welch, N.L., Carter, A., Metsky, H.C., Luo, C.Y., Abudayyeh, O.O., Gootenberg, J.S., *et al.* (2019). Programmable Inhibition and Detection of RNA Viruses Using Cas13. *Molecular cell* 76, 826-837 e811.

Gagnon, J.A., Obbad, K., and Schier, A.F. (2018). The primary role of zebrafish nanog is in extra-embryonic tissue. *Development* 145.

Gentsch, G.E., Spruce, T., Monteiro, R.S., Owens, N.D.L., Martin, S.R., and Smith, J.C. (2018). Innate Immune Response and Off-Target Mis-splicing Are Common Morpholino-Induced Side Effects in Xenopus. *Developmental cell* 44, 597-610 e510.

Gurtler, A., Kunz, N., Gomolka, M., Hornhardt, S., Friedl, A.A., McDonald, K., Kohn, J.E., and Posch, A. (2013). Stain-Free technology as a normalization tool in Western blot analysis. *Analytical biochemistry* 433, 105-111.

Haeussler, M., Schonig, K., Eckert, H., Eschstruth, A., Mianne, J., Renaud, J.B., Schneider-Maunoury, S., Shkumatava, A., Teboul, L., Kent, J., *et al.* (2016). Evaluation of off-target and on-target scoring algorithms and integration into the guide RNA selection tool CRISPOR. *Genome biology* 17, 148.

Halpern, M.E., Ho, R.K., Walker, C., and Kimmel, C.B. (1993). Induction of muscle pioneers and floor plate is distinguished by the zebrafish no tail mutation. *Cell* 75, 99-111.

Hamdane, N., Stefanovsky, V.Y., Tremblay, M.G., Nemeth, A., Paquet, E., Lessard, F., Sanij, E., Hannan, R., and Moss, T. (2014). Conditional inactivation of Upstream Binding Factor reveals its epigenetic functions and the existence of a somatic nucleolar precursor body. *PLoS genetics* 10, e1004505.

Hsu, P.D., Lander, E.S., and Zhang, F. (2014). Development and applications of CRISPR-Cas9 for genome engineering. *Cell* 157, 1262-1278.

Iwamatsu, T. (2004). Stages of normal development in the medaka *Oryzias latipes*. *Mechanisms of development* 121, 605-618.

Jao, L.E., Wente, S.R., and Chen, W. (2013). Efficient multiplex biallelic zebrafish genome editing using a CRISPR nuclease system. *Proceedings of the National Academy of Sciences of the United States of America* 110, 13904-13909.

Jing, X., Xie, B., Chen, L., Zhang, N., Jiang, Y., Qin, H., Wang, H., Hao, P., Yang, S., and Li, X. (2018). Implementation of the CRISPR-Cas13a system in fission yeast and its repurposing for precise RNA editing. *Nucleic acids research* 46, e90.

Joris, M., Schloesser, M., Baurain, D., Hanikenne, M., Muller, M., and Motte, P. (2017). Number of inadvertent RNA targets for morpholino knockdown in *Danio rerio* is largely underestimated: evidence from the study of Ser/Arg-rich splicing factors. *Nucleic acids research* 45, 9547-9557.

Kelly, A., and Hurlstone, A.F. (2011). The use of RNAi technologies for gene knockdown in zebrafish. *Briefings in functional genomics* 10, 189-196.

Kimmel, C.B., Ballard, W.W., Kimmel, S.R., Ullmann, B., and Schilling, T.F. (1995). Stages of embryonic development of the zebrafish. *Developmental dynamics : an official publication of the American Association of Anatomists* 203, 253-310.

Kinoshita M, Murata K., Naruse K., and Tanaka, M. (2012). *Medaka: Biology, Management, and Experimental Protocols*. (Wiley-Blackwell).

Kok, F.O., Shin, M., Ni, C.W., Gupta, A., Grosse, A.S., van Impel, A., Kirchmaier, B.C., Peterson-Maduro, J., Kourkoulis, G., Male, I., *et al.* (2015). Reverse genetic screening reveals poor correlation between morpholino-induced and mutant phenotypes in zebrafish. *Developmental cell* 32, 97-108.

Konermann, S., Lotfy, P., Brideau, N.J., Oki, J., Shokhirev, M.N., and Hsu, P.D. (2018). Transcriptome Engineering with RNA-Targeting Type VI-D CRISPR Effectors. *Cell* 173, 665-676 e614.

Kwan, K.M., Fujimoto, E., Grabher, C., Mangum, B.D., Hardy, M.E., Campbell, D.S., Parant, J.M., Yost, H.J., Kanki, J.P., and Chien, C.B. (2007). The Tol2kit: a multisite gateway-based construction kit for Tol2 transposon transgenesis constructs. *Developmental dynamics : an official publication of the American Association of Anatomists* 236, 3088-3099.

Lai, J.K.H., Gagalova, K.K., Kuenne, C., El-Brolosy, M.A., and Stainier, D.Y.R. (2019). Induction of interferon-stimulated genes and cellular stress pathways by morpholinos in zebrafish. *Developmental biology* 454, 21-28.

Laux, D.W., Febbo, J.A., and Roman, B.L. (2011). Dynamic analysis of BMP-responsive smad activity in live zebrafish embryos. *Developmental dynamics : an official publication of the American Association of Anatomists* 240, 682-694.

Lee, M.T., Bonneau, A.R., and Giraldez, A.J. (2014). Zygotic genome activation during the maternal-to-zygotic transition. *Annual review of cell and developmental biology* 30, 581-613.

Lee, M.T., Bonneau, A.R., Takacs, C.M., Bazzini, A.A., DiVito, K.R., Fleming, E.S., and Giraldez, A.J. (2013). Nanog, Pou5f1 and SoxB1 activate zygotic gene expression during the maternal-to-zygotic transition. *Nature* 503, 360-364.

Loosli, F., Winkler, S., Burgdorf, C., Wurmbach, E., Ansorge, W., Henrich, T., Grabher, C., Arendt, D., Carl, M., Krone, A., *et al.* (2001). Medaka eyeless is the key factor linking retinal determination and eye growth. *Development* 128, 4035-4044.

Lorenz, R., Bernhart, S.H., Honer Zu Siederdissen, C., Tafer, H., Flamm, C., Stadler, P.F., and Hofacker, I.L. (2011). ViennaRNA Package 2.0. *Algorithms for molecular biology : AMB* 6, 26.

Lund, E., Sheets, M.D., Imboden, S.B., and Dahlberg, J.E. (2011). Limiting Ago protein restricts RNAi and microRNA biogenesis during early development in *Xenopus laevis*. *Genes & development* 25, 1121-1131.

Ma, Z., Zhu, P., Shi, H., Guo, L., Zhang, Q., Chen, Y., Chen, S., Zhang, Z., Peng, J., and Chen, J. (2019). PTC-bearing mRNA elicits a genetic compensation response via Upf3a and COMPASS components. *Nature* 568, 259-263.

Mahas, A., Aman, R., and Mahfouz, M. (2019). CRISPR-Cas13d mediates robust RNA virus interference in plants. *Genome biology* 20, 263.

Malaga-Trillo, E., Solis, G.P., Schrock, Y., Geiss, C., Luncz, L., Thomanetz, V., and Stuermer, C.A. (2009). Regulation of embryonic cell adhesion by the prion protein. *PLoS biology* 7, e55.

Moreno-Mateos, M.A., Fernandez, J.P., Rouet, R., Vejnár, C.E., Lane, M.A., Mis, E., Khokha, M.K., Doudna, J.A., and Giraldez, A.J. (2017). CRISPR-Cpf1 mediates efficient homology-directed repair and temperature-controlled genome editing. *Nature communications* 8, 2024.

Moreno-Mateos, M.A., Vejnár, C.E., Beaudoin, J.D., Fernandez, J.P., Mis, E.K., Khokha, M.K., and Giraldez, A.J. (2015). CRISPRscan: designing highly efficient sgRNAs for CRISPR-Cas9 targeting in vivo. *Nature methods* 12, 982-988.

Mosimann, C., Kaufman, C.K., Li, P., Pugach, E.K., Tamplin, O.J., and Zon, L.I. (2011). Ubiquitous transgene expression and Cre-based recombination driven by the ubiquitin promoter in zebrafish. *Development* 138, 169-177.

Nagy, A., Gertsenstein, M., Vintersten, K., and Behringer, R (2003). *Manipulating the Mouse Embryo: A Laboratory Manual (3rd edition)* (Cold Spring Harbor Laboratory Press, Cold Spring Harbor).

Nasevicius, A., and Ekker, S.C. (2000). Effective targeted gene 'knockdown' in zebrafish. *Nature genetics* 26, 216-220.

Pauli, A., Montague, T.G., Lennox, K.A., Behlke, M.A., and Schier, A.F. (2015). Antisense Oligonucleotide-Mediated Transcript Knockdown in Zebrafish. *PloS one* 10, e0139504.

Robu, M.E., Larson, J.D., Nasevicius, A., Beiraghi, S., Brenner, C., Farber, S.A., and Ekker, S.C. (2007). p53 activation by knockdown technologies. *PLoS genetics* 3, e78.

Rossi, A., Kontarakis, Z., Gerri, C., Nolte, H., Holper, S., Kruger, M., and Stainier, D.Y. (2015). Genetic compensation induced by deleterious mutations but not gene knockdowns. *Nature* 524, 230-233.

Schulte-Merker, S., Hammerschmidt, M., Beuchle, D., Cho, K.W., De Robertis, E.M., and Nusslein-Volhard, C. (1994). Expression of zebrafish goosecoid and no tail gene products in wild-type and mutant no tail embryos. *Development* 120, 843-852.

Schulte-Merker, S., and Stainier, D.Y. (2014). Out with the old, in with the new: reassessing morpholino knockdowns in light of genome editing technology. *Development* 141, 3103-3104.

Sempou, E., Biasini, E., Pinzon-Olejua, A., Harris, D.A., and Malaga-Trillo, E. (2016). Activation of zebrafish Src family kinases by the prion protein is an amyloid-beta-sensitive signal that prevents the endocytosis and degradation of E-cadherin/beta-catenin complexes in vivo. *Molecular neurodegeneration* 11, 18.

Smith, I., Greenside, P.G., Natoli, T., Lahr, D.L., Wadden, D., Tirosh, I., Narayan, R., Root, D.E., Golub, T.R., Subramanian, A., *et al.* (2017). Evaluation of RNAi and CRISPR technologies by large-scale gene expression profiling in the Connectivity Map. *PLoS biology* 15, e2003213.

Smith, T.F., and Waterman, M.S. (1981). Identification of common molecular subsequences. *Journal of molecular biology* 147, 195-197.

Stainier, D.Y.R., Raz, E., Lawson, N.D., Ekker, S.C., Burdine, R.D., Eisen, J.S., Ingham, P.W., Schulte-Merker, S., Yelon, D., Weinstein, B.M., *et al.* (2017). Guidelines for morpholino use in zebrafish. *PLoS genetics* 13, e1007000.

Strahle, U., Blader, P., and Ingham, P.W. (1996). Expression of axial and sonic hedgehog in wildtype and midline defective zebrafish embryos. *The International journal of developmental biology* 40, 929-940.

Thisse, C., and Thisse, B. (2008). High-resolution in situ hybridization to whole-mount zebrafish embryos. *Nature protocols* 3, 59-69.

Veil, M., Schaechtle, M.A., Gao, M., Kirner, V., Buryanova, L., Grethen, R., and Onichtchouk, D. (2018). Maternal Nanog is required for zebrafish embryo architecture and for cell viability during gastrulation. *Development* 145.

Wang, Q., Liu, X., Zhou, J., Yang, C., Wang, G., Tan, Y., Wu, Y., Zhang, S., Yi, K., and Kang, C. (2019). The CRISPR-Cas13a Gene-Editing System Induces Collateral Cleavage of RNA in Glioma Cells. *Advanced science* 6, 1901299.

Weidinger, G., Stebler, J., Slanchev, K., Dumstrei, K., Wise, C., Lovell-Badge, R., Thisse, C., Thisse, B., and Raz, E. (2003). dead end, a novel vertebrate germ plasm component, is required for zebrafish primordial germ cell migration and survival. *Current biology : CB* 13, 1429-1434.

Wessels, H.-H., Méndez-Mancilla, A., Guo, X., Legut, M., Daniloski, Z., and Sanjana, N.E. (2020). Massively parallel Cas13 screens reveal principles for guide RNA design. *Nature biotechnology*, 1-6.

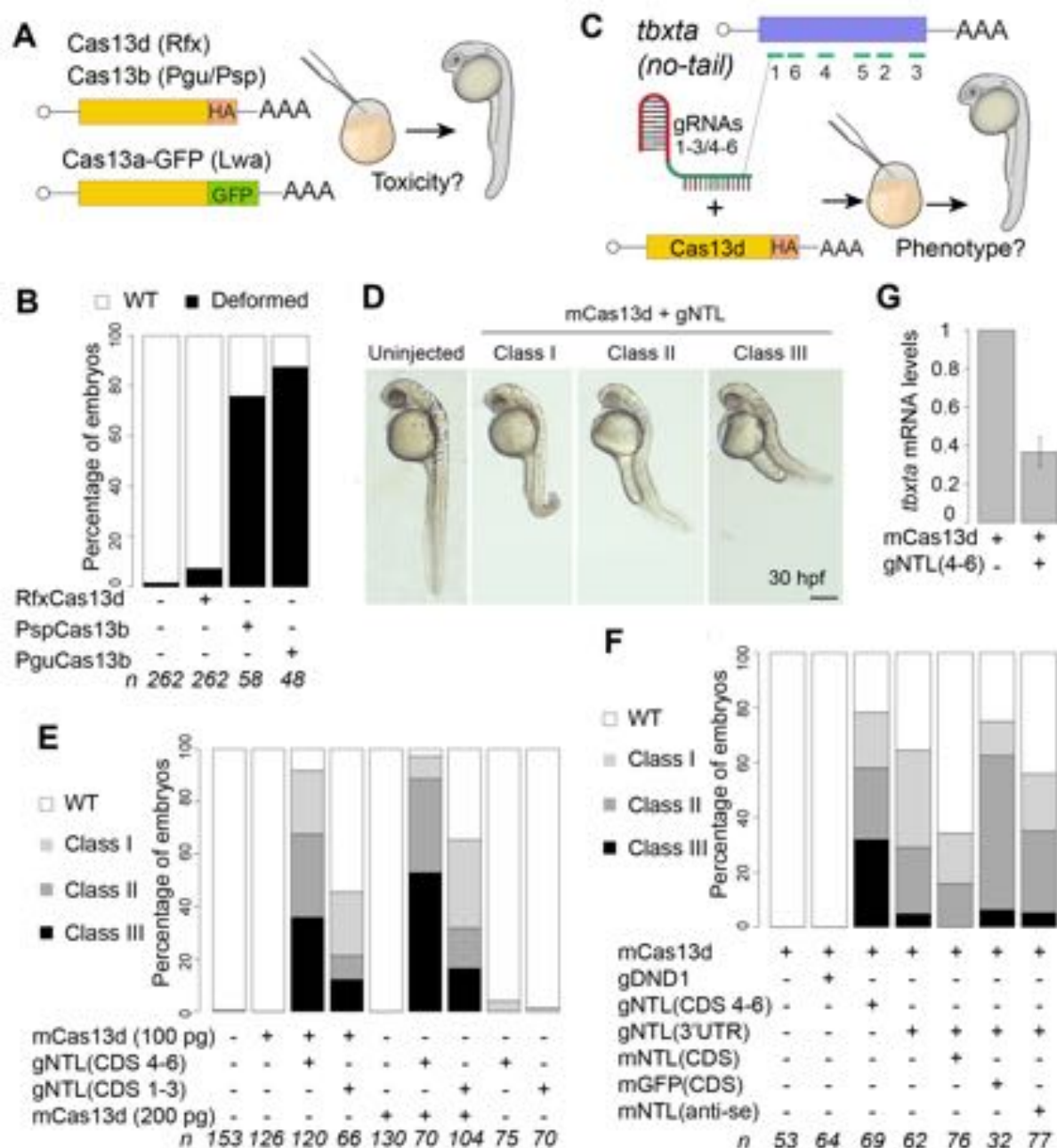
Westerfield, M. (1995). *The zebrafish book*, 3 edn (Eugene: The University of Oregon Press).

Wu, X., Sandhu, S., Patel, N., Triggs-Raine, B., and Ding, H. (2010). EMG1 is essential for mouse pre-implantation embryo development. *BMC developmental biology* 10, 99.

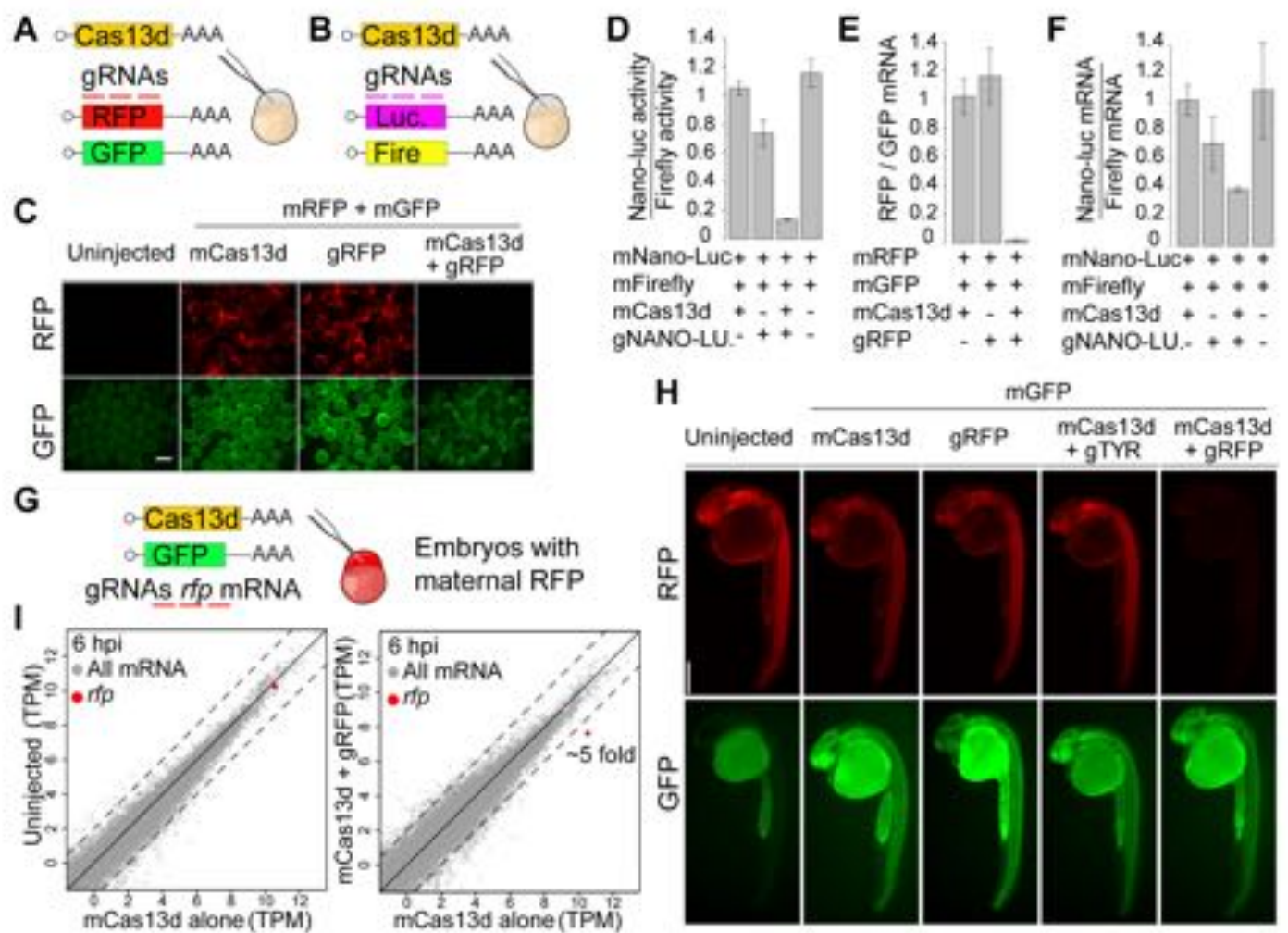
Yang, L.Z., Wang, Y., Li, S.Q., Yao, R.W., Luan, P.F., Wu, H., Carmichael, G.G., and Chen, L.L. (2019). Dynamic Imaging of RNA in Living Cells by CRISPR-Cas13 Systems. *Molecular cell* 76, 981-997 e987.

Zhou, H., Su, J., Hu, X., Zhou, C., Li, H., Chen, Z., Xiao, Q., Wang, B., Wu, W., Sun, Y., *et al.* (2020). Glia-to-Neuron Conversion by CRISPR-CasRx Alleviates Symptoms of Neurological Disease in Mice. *Cell*.

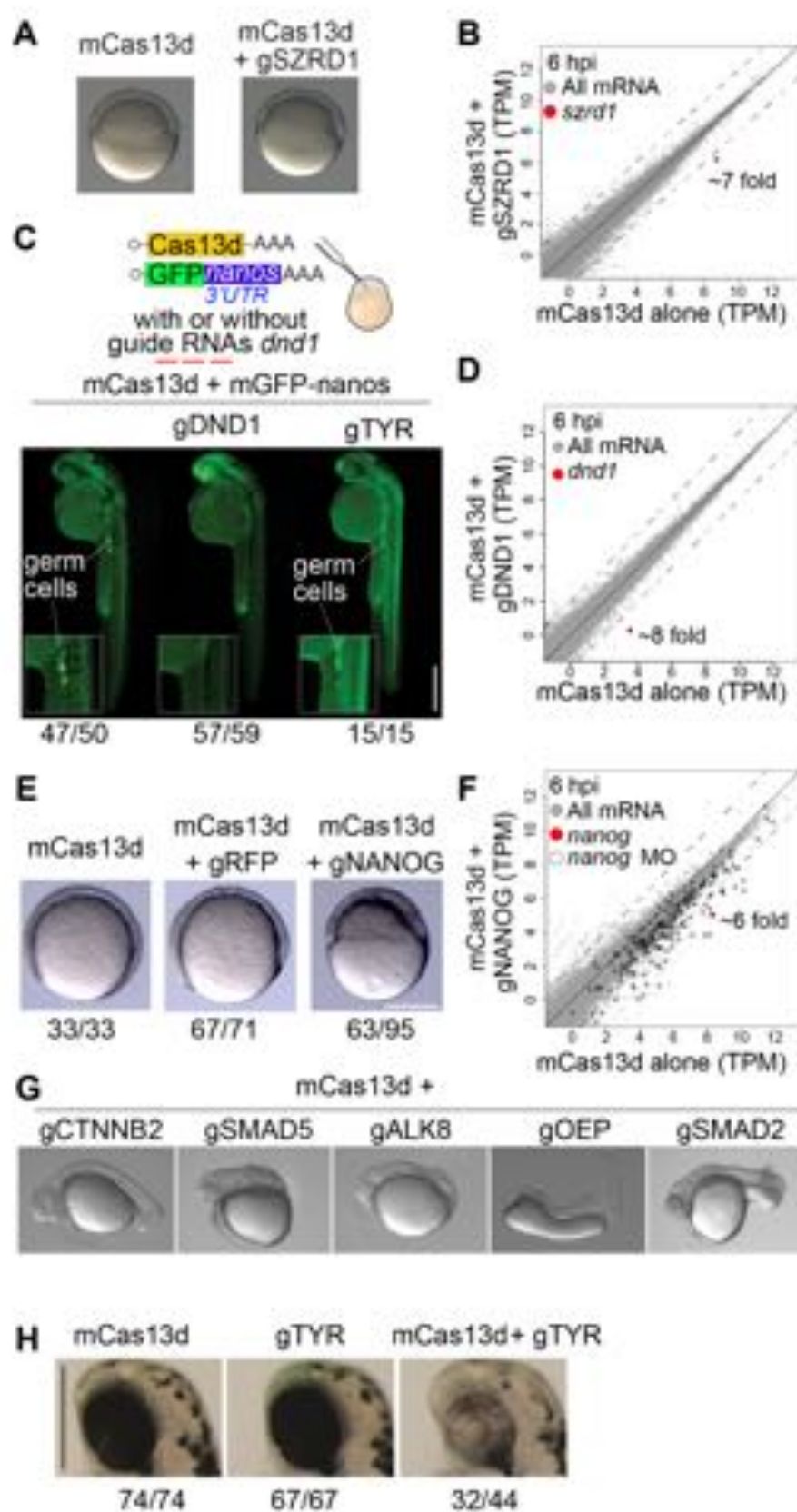
Kushawah et al., Figure 1



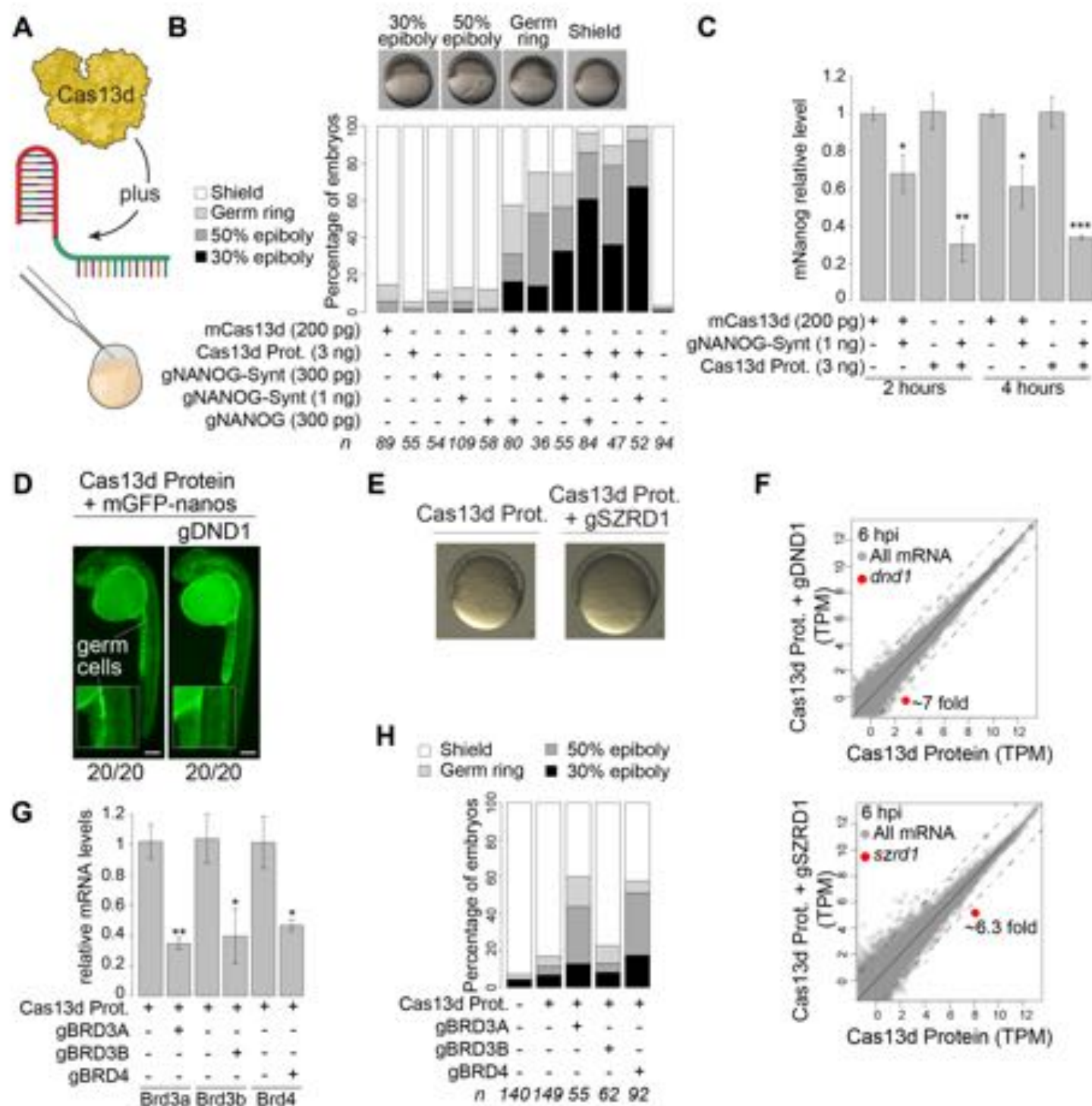
Kushawah et al., Figure 2



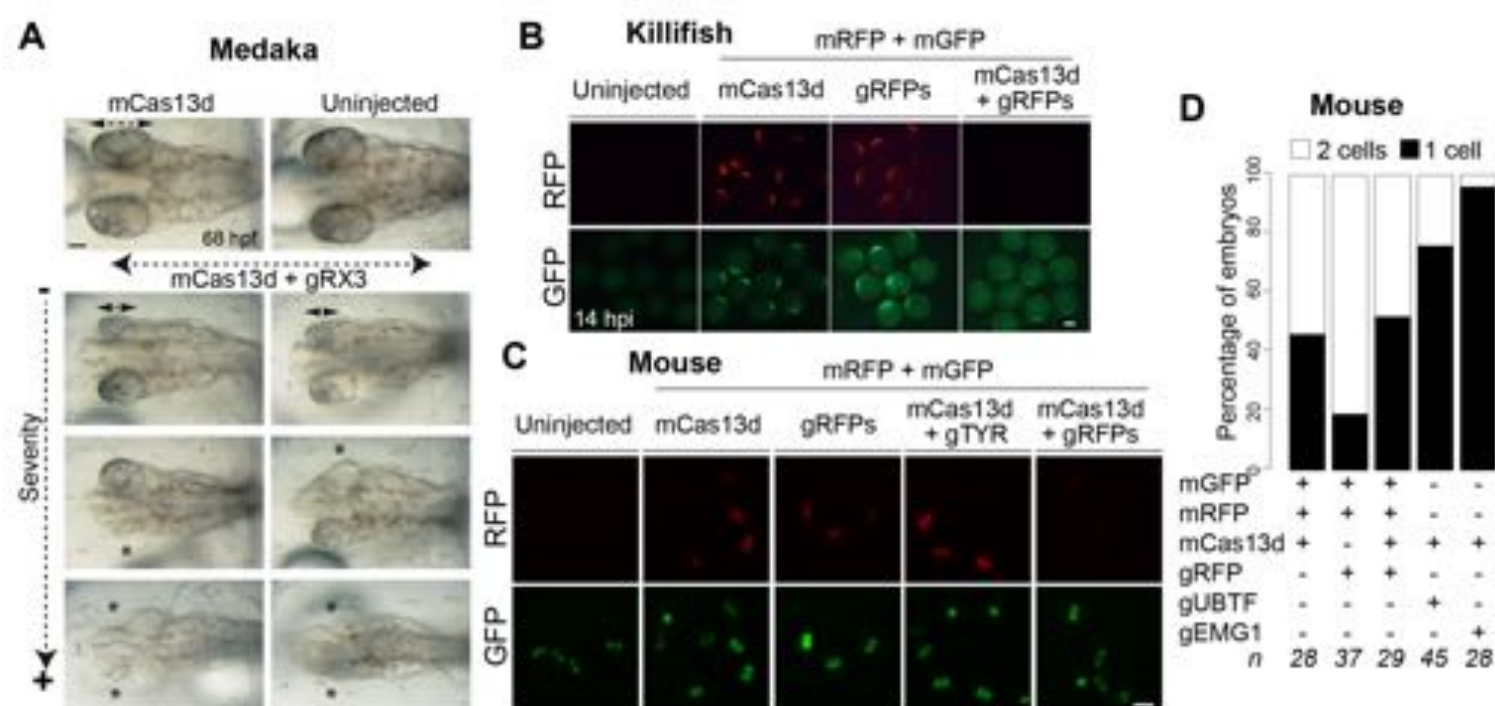
Kushawah et al., Figure 3



Kushawah et al., Figure 4



Kushawah et al., Figure 5

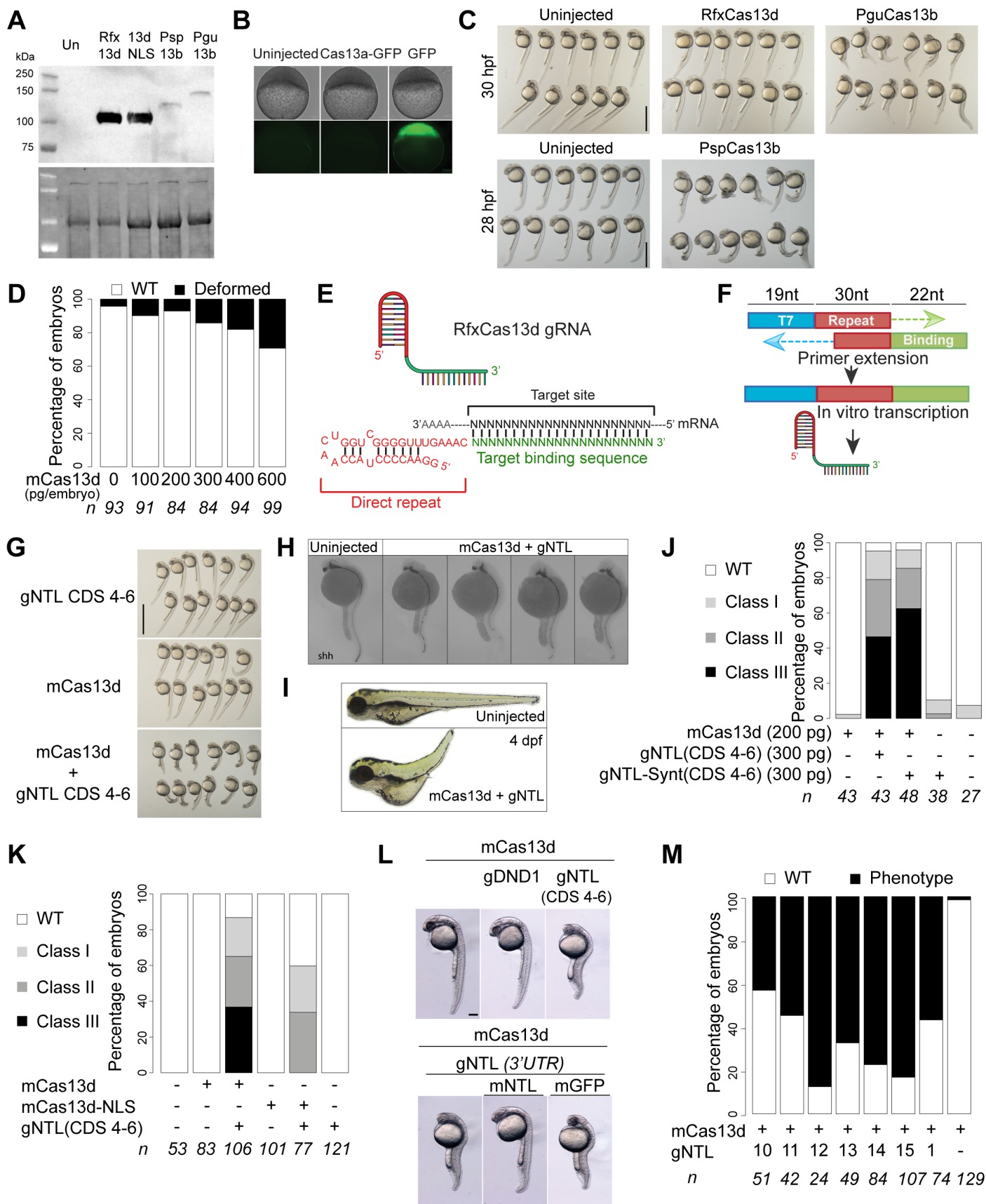


CRISPR-Cas13d induces efficient mRNA knock-down in animal embryos

Gopal Kushawah, Luis Hernandez-Huertas, Joaquin Abugattas-Nuñez del Prado, Juan R. Martinez-Morales, Michelle DeVore, Huzaifa Hassan, Ismael Moreno-Sanchez, Laura Tomas-Gallardo, Alejandro Diaz-Moscoso, Dahiana C. Monges, Javier R. Guelfo, William C. Theune, Emry O. Brannan, Wei Wang, Timothy J. Corbin, Andrea M. Moran, Alejandro Sánchez Alvarado, Edward Málaga-Trillo, Carter M. Takacs, Ariel A. Bazzini, Miguel A. Moreno-Mateos

Supplementary Information

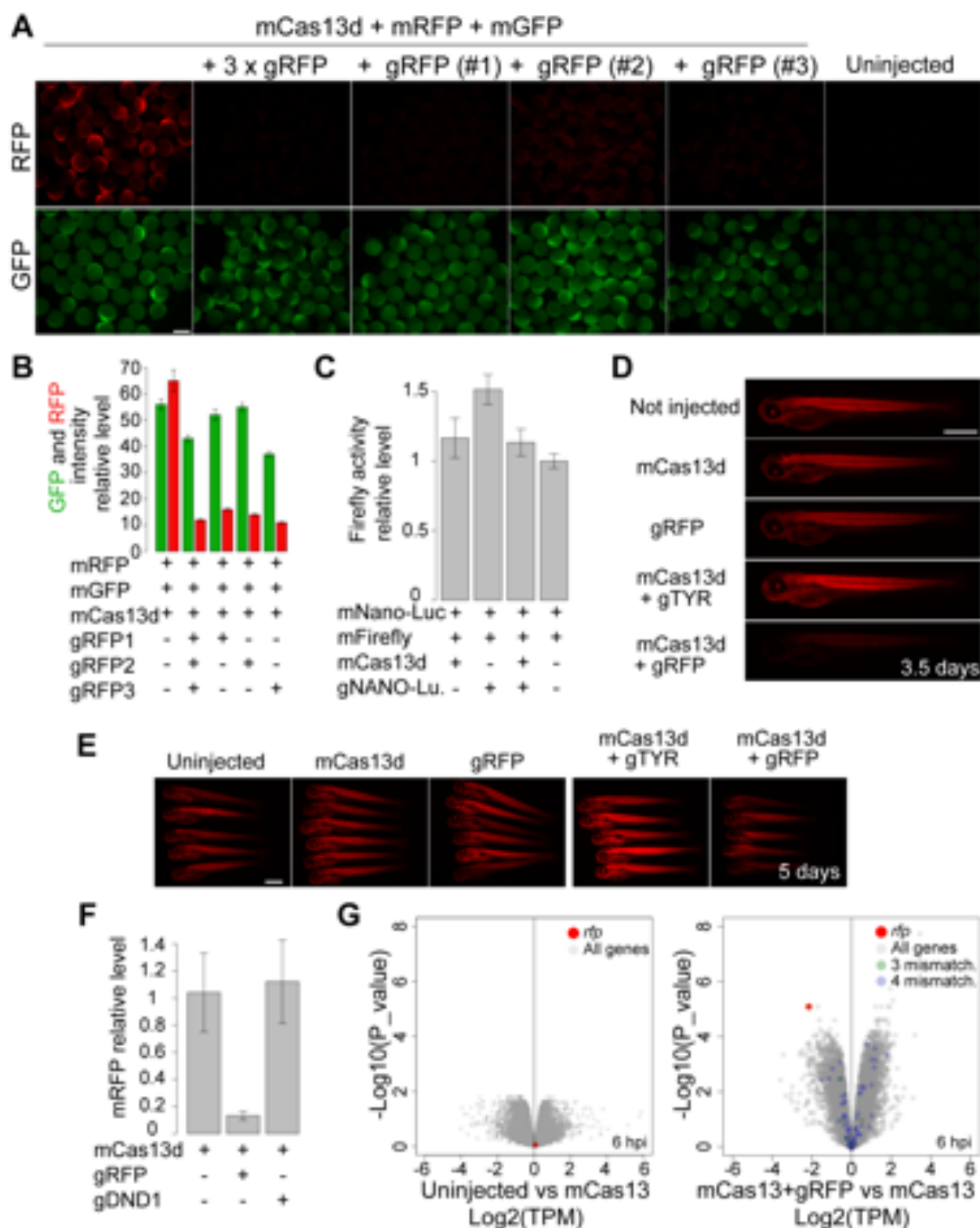
Kushawah et al., Figure Supplementary 1



Supplementary figure 1. CRISPR-Cas13 optimization in zebrafish, Related to Figure 1.

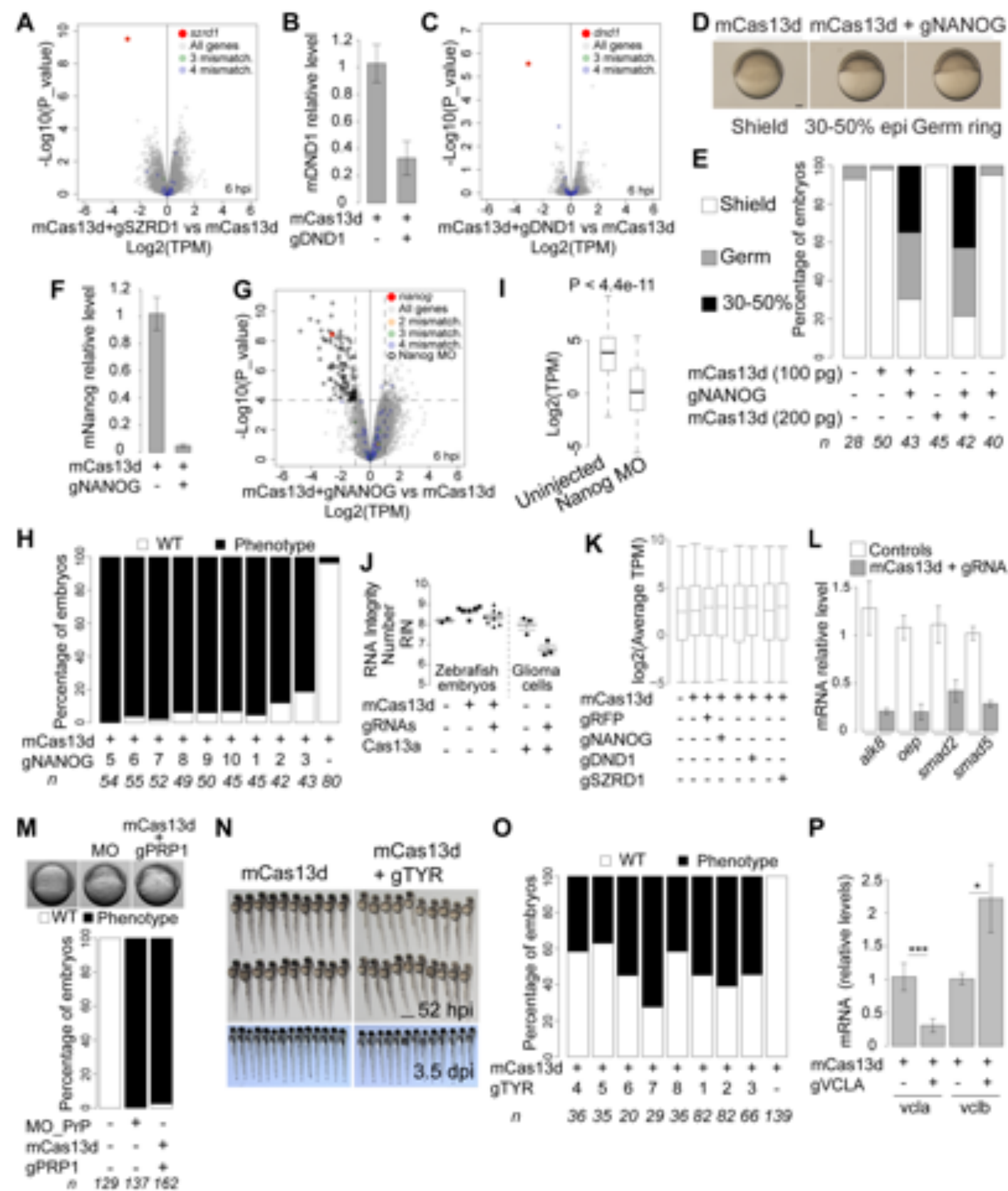
A) Western blot for HA showing protein level at 6 hours post injection (hpi) of the indicated Cas13 after injection of the encoding mRNA for each respective Cas13 mRNA into single cell zebrafish embryos (upper panel). Bottom panel shows Stain-Free signal (Gütler *et al.*, 2013) of the membrane before chemiluminescent detection (loading control). **B)** Representative pictures of embryos at 4.5 hours post fertilization (hpf) uninjected or injected with 200 pg of mRNA encoding for Lwa-Cas13a-GFP or GFP (scale bar, 0.1 mm). Lack of GFP expression was also observed using Cas13a-NLS-GFP version (not shown). **C)** Representative pictures of zebrafish embryos at 30 (top) or 28 (bottom) hpf uninjected or injected with 200 pg of mRNA encoding for RfxCas13d (mCas13d), PguCas13b or PspCas13b (scale bar, 1 mm). **D)** Toxicity evaluation of embryos. Stacked barplots showing the percentage of deformed and wild type (WT) zebrafish embryos (30 hpi) injected with different concentrations of mCas13d. Number of embryos evaluated (n) is shown for each condition. **E)** Schematic of gRNA structure for RfxCas13d (top) and scheme showing a gRNA (binding sequence in green, direct repeat in red) binding to the mRNA (black). Adapted from Moreno-Mateos *et al.*, 2017. **F)** Diagram of the gRNA generation by fill-in PCR followed by *in vitro* transcription. An oligonucleotide containing the T7 promoter (blue) followed by two Guanine and 30 nt of the direct repeat (in red) for annealing is used in combination with oligonucleotide containing 20 nt of the reverse complement of the repeat and 22 nt of the binding sequence (in green). Adapted from Moreno-Mateos *et al* 2017. **G)** Representative pictures of zebrafish embryos at 32 hpi injected with gRNAs targeting *tbxta* (gNTL 4-6;

300 pg/embryo) and/or mCas13d (200 pg/embryo) (scale bar, 1 mm). **H)** *In situ* hybridization for a notochord marker, *shh* mRNA, in embryos uninjected or injected with mCas13d (200 pg/embryo) and gNTL 4-6 (300 pg/embryo). Injected embryos display broadened and irregular *shh* expression, suggestive of compromised notochord formation. **I)** Picture of an uninjected embryo and a representative embryo injected with mCas13d (200 pg/embryo) and gNTL 4-6 (300 pg/embryo) at 4 dpf. **J)** Stacked barplots showing percentage of observed phenotypes in embryos injected with Cas13d mRNA alone or together with *in vitro* transcribed (gNTL) or chemically synthesized gRNAs (gNTL-Synt.) targeting *tbxta* mRNA at indicated amount of gRNA or mRNA injected per embryo. Knockdown classes are described in **Fig. 1D**. **K)** Stacked barplots showing percentage of observed phenotypes using gNTLs targeting CDS (gNTL 4-6, 300 pg/embryo) co-injected with mCas13d without (mCas13d) or with C- and N-terminal nuclear localization sites (mCas13d-NLS) (200 pg/embryo each mRNA). Knockdown classes are described in **Fig. 1D**. Number of embryos evaluated (n) is shown for each condition. **L)** Pictures of representative embryos from phenotype rescue experiment (**Fig. 1F**), injected with the indicated mRNA concentration and/or gRNAs (scale bar, 0.1 mm). **M)** Stacked barplots showing percentage of embryos with observed no tail phenotypes (similar to **Fig. 1D** but all classes were combined) injected with mCas13d (200 pg/embryo) alone or with individual gRNAs targeting *tbxta* gNTLs (300 pg/embryo). The gNTL numbers correspond to the sequence used (Table S1). Number of embryos evaluated (n) is shown for each condition.



Supplementary figure 2. CRISPR-RfxCas13d system efficiently targets reporter mRNAs in zebrafish, Related to Figure 2.

A) Fluorescence microscopy images of zebrafish embryos at 6 hours post injection with the indicated mRNA and gRNAs (scale bar, 0.5 mm). **B)** Barplot showing the relative intensity of GFP and RFP levels in the embryos injected with *gfp* and *rfp* mRNAs and with the indicated mCas13d and/or gRNAs at 6hpi for different combinations. **C)** Relative level of firefly luciferase activity at 6 hpi from the firefly luciferase mRNA injected as an internal control for each combination described in **Fig. 2D**. **D)** Fluorescence microscopy images showing the RFP intensity in the RFP transgenic fish at 3.5 and **E)** 5 days post injection using the indicated mRNA and/or gRNAs, suggesting time dependent recovery of RFP expression (scale bar, 0.1 mm). **F)** Barplot for the qRT-PCR analysis showing levels of *rfp* mRNA at 6 hpi in transgenic embryos injected with mCas13d alone or together with gRNAs targeting *dnd1* or *rfp* mRNAs. Results are shown as the averages \pm standard error of the mean from 2 independent experiments (n=20 embryos / experiment). *Taf15* mRNA was used as normalization control. **G)** Scatter plots representing the fold change in mRNA and the associated *p* value from two biological RNA-seq replicates at 6 hpi with the indicated gRNAs and/or mCas13d in RFP transgenic embryos. *Rfp* mRNA is indicated in Red. mRNAs that can potentially be recognized by used gRNAs, allowing up to 3 or 4 mismatches, are indicated in green and blue, respectively.



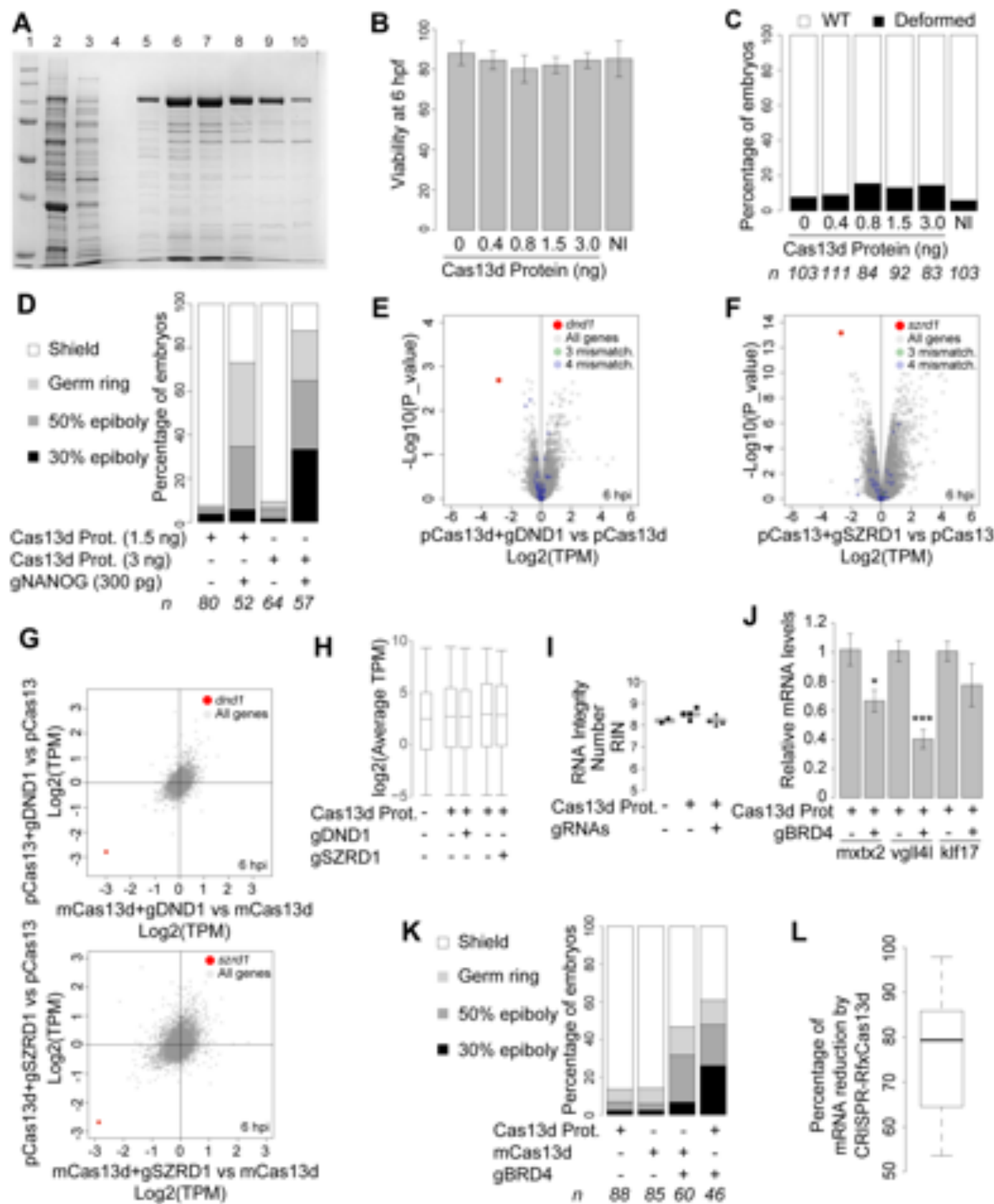
Supplementary figure 3. CRISPR-RfxCas13d system efficiently targets endogenous mRNAs in zebrafish, Related to Figure 3.

A) Scatter plots representing the fold change in mRNA and the associated p value from two biological RNA-seq replicates at 6 hours post injection with gRNAs targeting *szrd1* and/or mCas13d. *szrd1* mRNA is indicated in Red. mRNAs that can potentially be recognized by used gRNAs, allowing up to 3 or 4 mismatch, are indicated in green and blue, respectively. **B)** Barplot for the qRT-PCR analysis showing levels of *dnd1* mRNA in embryos at 6 hpi injected with mCas13d alone or together with gRNAs targeting *dnd1* mRNA. Results are shown as the averages \pm standard error of the mean from 2 independent experiments with 2 biological replicates per experiment ($n=20$ embryos/biological replicate). *Taf15* mRNA was used as normalization control ($p < 0.01$, t-test). **C)** Scatter plots representing the fold change in mRNA and the associated p value from two biological RNA-seq replicates at 6 hours post injection with gRNAs targeting *dnd1* and/or mCas13d. *Dnd1* mRNA is indicated in red. mRNAs that can potentially be recognized by used gRNAs, allowing up to 3 or 4 mismatches, are indicated in green and blue, respectively. **D)** Representative pictures of embryos injected with gRNAs targeting *nanog* CDS (200 pg per embryo injected at one-cell stage, gNANOG) and/or mCas13d (100 or 200 pg per embryo injected at one-cell stage) showing different developmental stages. Shield, germ ring and 30-50% epiboly (30-50% epi) correspond to 6, 5.7 and 5.3-4.7 hpf in wild type embryos growing in standard conditions, respectively (scale bar, 0.1 mm.) **E)** Stacked barplots showing percentage of observed phenotypes under the conditions described. Number of embryos evaluated (n) is shown for each condition. **F)** Barplot for the qRT-PCR analysis showing levels of *nanog* mRNA

in embryos at 6 hpi injected with mCas13d alone or together with gRNAs targeting *nanog* mRNA ($p < 0.0001$, t-test). Results are shown as the averages \pm standard error of the mean 2 independent experiments with at least 2 biological replicates each (n=20 embryos/ biological replicate). *Taf15* mRNA was used as normalization control. **G)** Scatter plots representing the fold change in mRNA and the associated p value from two biological RNA-seq replicates at 6 hours post injection with gRNAs targeting *nanog* and/or mCas13d. *Nanog* mRNA is indicated in red. Dashed lines indicate more than 4-fold differences between in RNA level and p adjusted value = $1e4$). mRNAs that can potentially be recognized by used gRNAs, allowing up to 2, 3 or 4 mismatches, are indicated in orange, green and blue, respectively. Black outline indicates mRNA that display reduced expression (>2 -fold decrease and p adjusted value $< 1e4$) due to the injection of mCas13d with gRNAs targeting *nanog*. **H)** Stacked barplots showing percentage of observed *nanog* phenotypes (similar to panel **E** but all type of developmental delayed were combined) in embryos injected with mCas13d (200 pg/embryo) alone or with individual gRNAs targeting *nanog* mRNA (300 pg/embryo). The gNANOG numbers correspond to the sequence used (Table S1). Number of embryos evaluated (n) is shown for each condition. **I)** Boxplot showing that the mRNAs down regulated in the embryos injected with mCas13d with gRNAs targeting *nanog* mRNA (black outline in panel G) also display lower mRNA level in embryos injected with morpholino targeting *nanog* expression compare to uninjected embryos ($p < 4.4e-11$, Mann–Whitney U -test). The box defines the first and third quartiles, with the median indicated with a thick black line and vertical lines indicate the variability outside the upper and lower quartiles. **J)** RNA integrity numbers (RIN) from RNA samples used for

RNA-seq from uninjected and injected zebrafish embryos with mCas13d alone or with gRNAs determined by Agilent Bioanalyzer 2100. The RIN reported in human cells treated with Cas13a are also shown (Wang et al., 2019) ($p > 0.08$, comparing all zebrafish samples between them, $p < 0.021$ for glioma cells, respectively; one-way ANOVA). **K)** Boxplot showing non-significant differences at the mRNA level between the uninjected and injected embryos with mCas13d with or without gRNAs of 289 mRNA that were previously shown to be differentially expressed genes between morphants and uninjected or buffer-injected embryos (Lai et al., 2019) ($p > 0.59$, Wilcoxon signed-rank test). **L)** Barplot for the qRT-PCR analysis showing levels of *alk8*, *oep*, *smad2* and *smad5*, mRNAs in embryos at 6 hpi. Results are shown as the averages \pm standard error of the mean from 3 biological replicates. ($n = 20$ embryos/biological replicate). (*alk* $p < 0.00011$; *oep* $p < 1.42 \times 10^{-5}$, *smad2* $p < 0.0013$, *smad5* $p < 3.43 \times 10^{-6}$, t-test). **M)** Representative pictures of embryos uninjected and injected at one-cell stage with a morpholino (MO) or three gRNAs (300 pg per embryo injected at one-cell stage, gPRP1) targeting *prp1* mRNA and mRNA (200 pg per embryo). Stacked barplots showing percentage of embryos with epibolic arrest (phenotype) for the three conditions indicated. Number of embryos evaluated (n) is shown for each condition. **N)** Representative pictures of zebrafish embryos from the experiment described in **Fig. 3H** (scale bar, 1 mm) at 2 (upper) and 3.5 (lower) days post fertilization. **O)** Stacked barplots showing percentage of embryos with a reduced pigmentation by injection of mCas13d (200 pg/embryo) alone or with individual gRNAs targeting *tyr* mRNA (300 pg/embryo). The gTYR numbers correspond to the sequence used (Table S1). Number of embryos evaluated (n) is shown for each condition. **P)** Barplot for qRT-PCR showing

significant knockdown of *vc/a* mRNA and higher level of *vc/b* mRNA by co-injection of mCas13d with three gRNAs targeting *vc/a* mRNA, indicating that CRISPR-Cas13 system can trigger gene compensation. Results are shown as the averages \pm standard error of the mean from at least 3 biological replicates from 2 independent experiments ($p^* < 0.05$, $*** < 0.001$, t-test) (n=20 embryos/biological replicate).

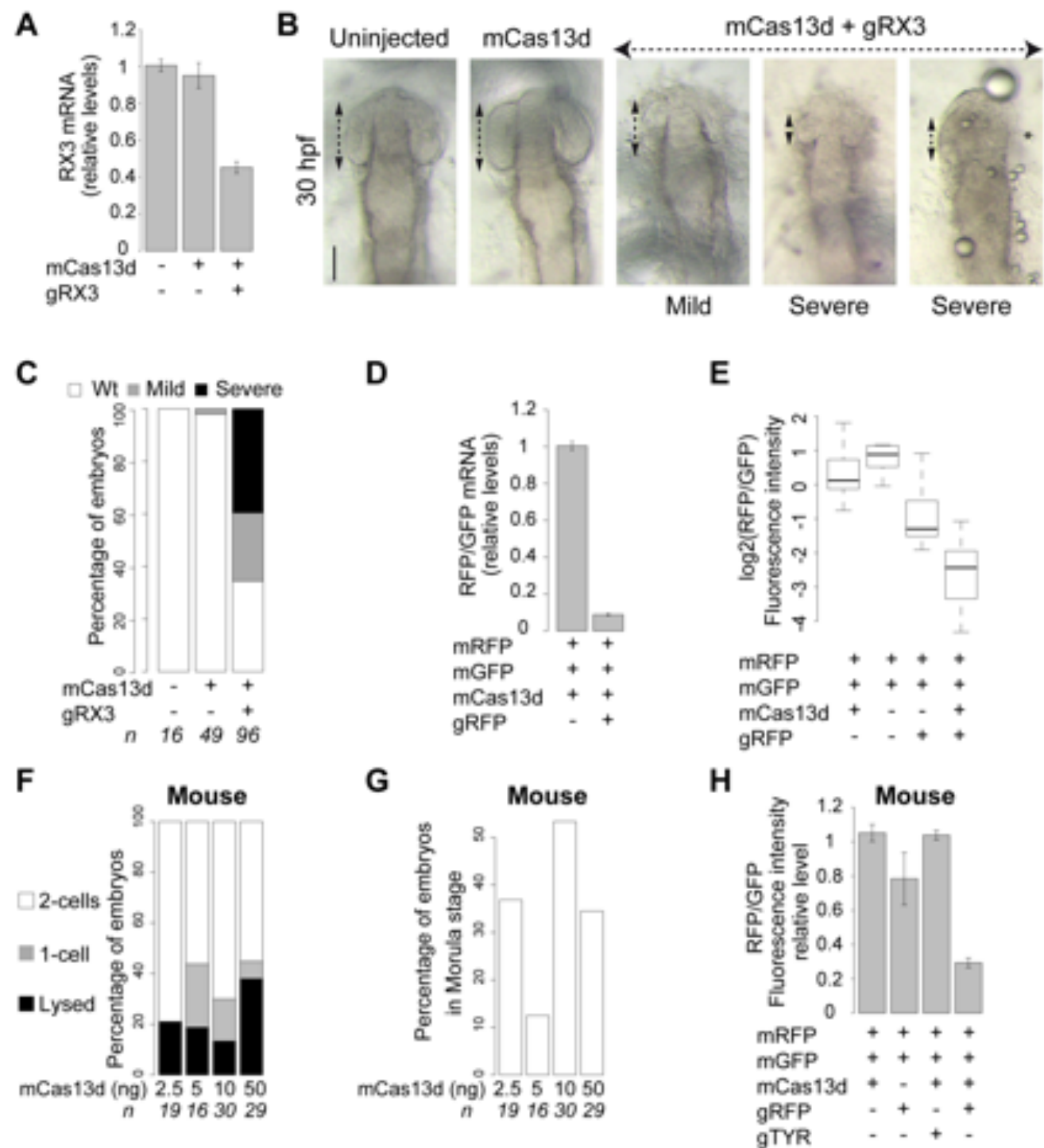


**Supplementary Figure 4. RfxCas13d protein enhances maternal RNA targeting,
Related to Figure 4.**

A) SDS-PAGE of Cas13d purification process. Coomassie blue stained 10% SDS-PAGE. Lane 1: Precision Plus Protein™ All Blue Pre-stained Protein Standards (BioRad). Lane 2: Lysate before HisTrap FF column chromatography. Lane 3: Flow through after column chromatography. Lane 4: Column wash before elution. Lanes 5-10: Fractions 6, 7, 8, 10, 12 and 14 of the imidazole gradient elution. Fractions 8-14 were selected for dialysis of the imidazole gradient elution. **B)** Barplots showing the viability of embryos at 6 hpi after the injection of different concentration of Cas13d protein (Cas13d protein) into one-cell stage zebrafish embryos. Results are shown as the averages \pm standard error of the mean from three independent experiments. At least 40 embryos were injected per condition and experiment. No significant differences were found between tested conditions (one-way ANOVA). **C)** Stacked barplots showing the percentage of deformed and wild type (WT) zebrafish embryos 24 hpi with the indicated amount of Cas13d. **D)** Stacked barplots showing percentage of observed phenotypes in embryos injected with purified Cas13d protein at different concentration, alone or together with *in vitro* transcribed gRNAs (gNANOG) targeting *nanog* mRNA. Indicated amount of gRNA or protein is per injected embryo. Knockdown phenotype classes are described in **Fig.4B** (upper panel). Number of embryos evaluated (n) is shown for each condition ($p < 0.0014$, Chi-square 1.5 ng plus gRNA vs 3 ng plus gRNA). **E) F)** Scatter plots representing the fold change in mRNA level and the associated p value from two biological RNA-seq replicates at 6 hours post injection with Cas13d protein alone or with gRNAs targeting **E)** *dnd1* or **F)** *szrd1*. *dnd1* and *szrd1* mRNAs are indicated in red in

each respective panel. mRNAs that can potentially be recognized by used gRNAs, allowing up to 3 or 4 mismatches, are indicated in green and blue, respectively. **G)** Scatter plot representing the fold change in mRNA level between embryos injected with mCasd13d alone or co-injected with mCas13d and gRNAs targeting *dnd1* (upper panel) or *szrd1* (lower panel) mRNAs (x axis) and embryos injected with Cas13d protein alone or with the same respective gRNAs (y axis). *dnd1* or *szrd1* are indicated in red in their respective panels. **H)** Boxplot showing non-significant differences at the mRNA level between the uninjected and injected embryos with Cas13d protein with or without gRNAs of 289 mRNA that were previously shown to be differentially expressed genes between morphants and uninjected or buffer-injected embryos (Lai et al., 2019) ($p > 0.7$, Wilcoxon signed-rank test). **I)** RNA integrity numbers (RIN) from RNA samples used for RNA-seq from uninjected and injected zebrafish embryos with Cas13d protein alone or with gRNAs determined by Agilent Bioanalyzer 2100. The uninjected zebrafish embryos samples are share with Supplementary Figure 3J ($p > 0.09$, comparing all samples between them; one-way ANOVA). **J)** Barplots for qRT-PCR analysis showing the relative levels of *mxtx2*, *vgll4l* and *klf17* mRNAs in embryos at 4 hpi with Cas13d protein (3 ng/embryo) alone or together with gRNAs (300 pg/embryo) targeting *brd4* mRNAs. Results are shown as the averages \pm standard error of the mean from 4 biological replicates from two independent experiments ($p^* < 0.05$, $*** < 0.001$, t-test) (n=10 embryos/biological replicate). **K)** Stacked barplots showing percentage of observed phenotypes in embryos injected with Cas13d mRNA or protein, alone or together with gRNAs targeting Brd4. Number of embryos evaluated (n) is shown for each condition. The phenotype selection criteria were the same as in **Fig. 4B**. **L)** Boxplot showing the

percentage of mRNA reduction by the CRISPR-RfxCas13d system for each targeted mRNA using Cas13d mRNA or protein measured by RNA-seq or qRT-PCR.



Supplementary figure 5. CRISPR-RfxCas13d targets different mRNAs in animal models, Related to Figure 5.

A) Barplot for the qRT–PCR analysis showing levels of *rx3* mRNA in medaka embryos at 21 hpi injected with mCas13d alone or together with gRNAs targeting *rx3* mRNA. Results are shown as the averages \pm standard error of the mean from 2 (uninjected embryos) or 3 biological replicates (two technical replicates per biological replicate). *actin-beta* mRNA was used as normalization control. The data were subjected to one-way ANOVA test. **B)** Representative pictures of medaka embryos at 30 hpi injected in the conditions described in **Fig. 5A** and showing different grade of severity of the phenotype. Double arrows and asterisk indicate eye length and absence of eye, respectively (scale bar, 0.1 mm). **C)** Stacked barplots showing percentage of observed medaka phenotypes at 30 hpi (**panel A**) under injection conditions described in **Fig. 5A**. Number of embryos evaluated (n) is shown for each condition. **D)** Barplot for the qRT–PCR analysis showing levels of *rfp* mRNA with respect to mGFP levels in Killifish embryos injected with *rfp*, *gfp* and Cas13d (mCas13d) mRNAs with or without gRNAs targeting *RFP* mRNA. Results are shown as the averages \pm standard error of the mean from 2 biological replicates ($p < 0.0081$, t-test) (n=20 embryos/biological replicate) **E)** Boxplot showing the logarithmic ratio between the RFP and GFP fluorescence intensity observed in killifish embryos (at least 14 embryos per condition) from two independent experiments with the indicated mRNA and/or gRNAs at 14 hpi. The RFP/GFP intensity ratio was compared between control condition (mCas13d alone) vs without mCas13 or gRNAs (mRFP and mGFP only), gRFP alone and mCas13d plus gRFP, ($p = 0.5547$, $p < 0.0137$ and $p < 0.0001$, respectively; Krushal-Wallis test). The box defines the first and

third quartiles, with the median indicated with a thick black line and vertical lines indicate the variability outside the upper and lower quartiles. **F)** Stacked plots showing the percentage of mouse embryos at 1 or 2 cells stage or lysed after 24 hours post injection with 1-2 pl of the indicated mCas13d concentration. The number of embryos (n) is indicated for each condition. **G)** Barplot showing the proportion of embryos injected with different mCas13d concentration that reach Morula stage. The number of embryos (n) is indicated for each condition. **H)** Barplot showing the RFP/GFP intensity ratio in mouse embryos from two independent experiments (at least 23 embryos per condition) injected with the mRNAs encoding for RFP and GFP and with the indicated mCas13d and/or gRNA at 24 hours post injection. The RFP/GFP intensity ratio was compared between control condition (mCas13d alone) vs gRFP alone, mCas13d plus gTYR and mCas13d plus gRFP ($p < 0.0132$, $p = 0.8954$ and $p < 0.0001$, respectively; Krushal-Wallis test).